Abstract

A zeolitic material synthesized from coal fly ash (Na-Ze) was modified to magnesium (Mg-Ze) and magnesium-potassium (Mg/K-Ze) forms for being used as a sorbent material to enhance simultaneous removal of ammonium and phosphate from wastewater effluents. Loaded zeolites can be used afterwards as slow-release fertilizers or in soil quality improving actions.

A series of batch experiments were carried out in order to determine the sorption capacity and kinetic performance of zeolites. Once these results were obtained a new set of experiments were performed with the objective of setting up a hybrid ultrafiltration-adsorption pilot plant using zeolite as a sorbent material in a more realistic conditions of wastewater treatment plant.

Equilibrium, kinetic, and zeolite dose studies were carried out through batch experiments in NH_4^+/PO_4^{3-} binary systems. All equilibrium experimental data were fitted by Langmuir isotherm model, and maximum sorption capacities of ammonium and phosphate were determined for both zeolites. q_m of Mg-Ze was reported to be 30.90 mg·g^{-1} and 12.41 mg·g^{-1} for ammonium and phosphate, respectively, while results for Mg/K-Ze were 27.79 mg·g^{-1} and 57.87 mg·g^{-1}. Kinetics was overall reported to be very swift, reaching the equilibrium of ammonium sorption in less than 2 minutes. For the phosphate, sorption was slower and long-termed. The optimum zeolite dose for nutrient removal was determined to be 2 g/dm^3.

Finally, after a successful experiment at the UF-adsorption pilot plant, global mass removal efficiency of ammonium and phosphate from a simulated wastewater sample was reported to be 60% and 90%, respectively.

ETSEIB

ETSEIB

Nutrient recovery from wastewater by adsorption on Magnesium/Potassium zeolites
in adsorption-ultrafiltration hybrid systems

Page 3

INDEX

ETSEIB

ETSEIB

1. Glossary

EDS   Energy Dispersive X-Ray Spectroscopy

K   Potassium

MAP   Magnesium Ammonium Phosphate

Mg   Magnesium

Na   Sodium

NF   Nanofiltration

q_m   Maximum sorption capacity

SEM   Scanning Electron Microscopy

STR   Stirred Tank Reactor

S/L   Solid/Liquid ratio

UF   Ultrafiltration

WWTP   Wastewater Treatment Plant

Ze   Zeolite

ZFA   Zeolite synthesized from fly ashes

ETSEIB

2. Foreword

2.1. Origin of the project

This Final Degree Project is part of a PhD. thesis carried out by Xialei You about removal and recovery of nutrients from wastewater through different separation technologies e.g. adsorption and membrane technology. Different sorbents and mechanisms are being studied at the present time by students and professors from the Chemical Engineering Department of the ETSEIB (Escola Tècnica Superior d'Enginyeria Industrial de Barcelona), at the UPC (Universitat Politècnica de Catalunya).

2.2. Motivation

Nowadays are critical times for the global society. Harvesting and providing food for the whole world population entails a strong investment of money and effort in fertilizers industry. There is an unprecedented increasing demand of synthetic fertilizers, and natural resources are not able to cope with this global need of production.

Moreover, clean water is scarce and has become a precious good worldwide, so it is necessary to decontaminate wastewaters from all kind of pollutants and especially nitrogen and phosphorus compounds, which might have an added value as fertilizer components.

From that point of view, the goal of satisfying this need and aiming for a global growth and improvement are the drivers to perform this project and researching for new ways to recover nutrients from wastewater.

2.3. Previous work

This study is a continuation of a research started by Xialei You and carried out by other students in previous bachelor degree projects and master thesis. In those works, the performance of different kinds of polymeric sorbents as well as different salt modified zeolites on nutrient recovery from wastewater has been studied.

ETSEIB

3. Introduction

3.1. Objectives

The main objective of this project is to recover simultaneously NH_4^+ and PO_4^{3-} from wastewater by using salt modified zeolites.

Aiming to achieve this main goal, several tasks have been proposed:

- To perform the modification of provided sodium synthetic zeolite (Na-Ze) onto the magnesium/potassium (Mg/K-Ze) and magnesium (Mg-Ze) forms.
- To carry out a series of batch experiments with the modified zeolite in order to report the zeolite's maximum sorption capacity, kinetic performance as well as the optimum solid/liquid ratio that maximizes nutrients removal efficiency.
- To remove nutrients in a hybrid ultrafiltration-adsorption pilot plant, in order to report a deeper analysis of the modified zeolite in a more realistic conditions.

3.2. Scope of the project

This project does not focus in making experimental studies only at laboratory scale, but also in working at a larger scale such as an adsorption-ultrafiltration hybrid pilot plant. Thus, the adsorption process of ammonium and phosphate is analyzed beyond batch experiments (equilibrium and kinetic), by working with an UF-adsorption pilot plant in which an ultrafiltration membrane is used to separate the zeolite from the stream leaving the adsorption reactor.

ETSEIB

ETSEIB

4. State of the art

Phosphorus and Nitrogen are essential elements for life on Earth as they are necessary for plant growth (Huang, Jiang & Ding, 2014). However, excess of these nutrients in aquatic systems may drive an ecosystem to eutrophication due to a massive growth of the biomass that consumes all remaining oxygen in the environment. This phenomenon entails a progressive decrease of the availability of these elements as they become accumulated on lakes, rivers and swamps.

Nitrogen and specially Phosphorus are elemental for the production of fertilizers, detergents, processed food and many other P-based and N-based chemicals (Van Vuuren et al., 2010). Depletion of Nitrogen reserves are not a cause of concern since it is an abundant element in nature, but Phosphorus is generally mined from quarries of natural P minerals (apatite, P_2O_5...) and these reserves will run out in a couple of centuries if no recycling routes are implemented (Huang, Jiang & Ding, 2014).

According to the US Geological Survey Mineral Resources Program, world resources of phosphate rock are more than 300 billion tons (USGS, 2015). However, it was estimated that there are 11,000 million tons of phosphate rocks that economically cannot be processed at present (Shu et al., 2006).

Moreover, approximately 21.4 Mt of phosphorus were extracted in 2009 from phosphate rock mining operations (Koppelaar & Weikard, 2013) and nowadays phosphate rock consumption has become even larger as consumption of P_2O_5 contained in fertilizers was 42.2 Mt in 2014 and it was projected to increase to 45.9 Mt in 2018 (USGS, 2015), to 47.6 Mt in 2020 and to 83.7 Mt in 2050 (Tilman et al., 2001). Figure 4-1 shows a demand simulation of phosphorus resources in forthcoming decades.
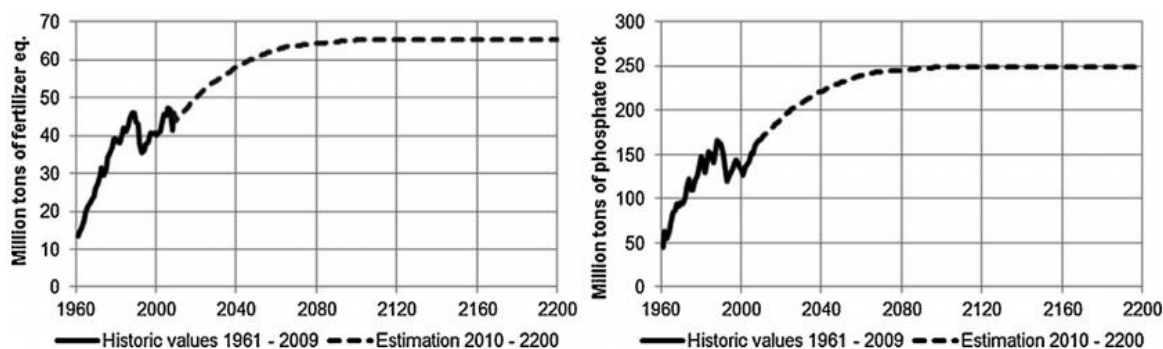
Figure 4-1. Result demand simulation from 2010 to 2200 without supply constraint for fertilizer equivalent (fertilizer + non-fertilizer use), on left as tone of fertilizer (46% P), and on right as phosphate rock (Koppelaar & Weikard, 2013)

Many solutions have been studied for this problem of worldwide concern. Any technology to recover phosphorus and nitrogen shall not only prevent eutrophication but also conserve limited natural resources. Therefore, not only a way to improve fertilizers' performance and efficiency is sought, but also many technologies are in constant development to recover these nutrients from wastewater effluents, such as for example biological treatments, precipitation, filtration and adsorption methods.

4.1. Removal and recovery technologies for ammonium and phosphate from wastewater

Removing Nitrogen and Phosphorus species from waste water is one the objectives of wastewater treatment plants (WWTPs).

Nitrogen is generally found in wastewater as ammonia, nitrate, nitrite and other organic nitrogen substances. Then, mostly oxidation-based biological treatments are used to remove nitrogen species from water.

By its side, Phosphorus is present in the form of orthophosphate, polyphosphate and organic bound phosphorus, so precipitation methods are usually also effective because of the phosphates, although organic species are still majority.

However, resulting streams from secondary wastewater treatments are generally already treated from organic compounds, and most of the remaining N and P are present in their ionic aqueous form: ammonium and phosphate (NH_4^+ and PO_4^{3-}). Generally, two kinds of reagents must be applied then for the removal of NH_4^+ and PO_4^{3-}. For example, the

Nutrient recovery from wastewater by adsorption on Magnesium/Potassium zeolites
in adsorption-ultrafiltration hybrid systems

Page 13

combination of a cation exchanger and an anion exchanger, or a cation exchanger and an inorganic cohesion precipitant (Wu et al., 2006). Thus, NH_4^+ is normally substituting a cation (Na^+, K^+, Mg^{2+}, Ca^{2+}, …) through ionic exchange, while PO_4^{3-} is generally driven into crystallization as struvite (MAP, $NH_4MgPO_4 \cdot 6H_2O$) through precipitation methods.

4.1.1. Biological treatment

Biological processes use microorganisms to remove dissolved nitrogen and phosphorus from wastewater. Most of these processes are based in the oxidation of biological carbon and nitrogen as well as in the removal of nutrients in the form of phosphoric and ammonium. Phosphoric nutrients are removed by aerobic digestion of bacteria, whose cells feed on orthophosphates to grow and to multiply, and nitrogen is removed by nitrification and denitrification processes.

Nitrification consists of the oxidation of ammonium (NH_4^+) to nitrite (NO_2^-) followed by the oxidation of nitrite to nitrate (NO_3^-). After that, denitrification is responsible of reducing nitrate into nitrogen gas (N_2) using electrons donated by an organic matter. Both nitrification steps are respectively carried out by ammonium oxidation bacteria (AOB) and nitrite oxidation bacteria (NOB), which consume oxygen during the process, while denitrification is just requiring organic matter as electron donator (Ma et al., 2016).

However, there are alternative ways to enhance nitrogen removal. Autotrophic nitrogen removal technology, which can remove nitrogen without using organic matter, is considered to be a more sustainable way for wastewater treatment (Ma et al., 2016) and it can be achieved by anaerobic ammonium oxidation process (anammox), which was thought to be a promising way of making sewage treatment energy-neutral or energy-generating (Kartal et al., 2010). In fact, anammox oxidation bacteria oxidize ammonium using nitrite as an electron acceptor, producing N_2 under anoxic conditions. As such, biological nitrogen can be removed through nitritation/anammox and partial-denitrification/anammox (Figure 4-2).

Therefore, organic matter is not needed at all for anammox nitrogen removal, and it could alternatively be used to produce biogas (methane) to enhance energy recovery from wastewater.
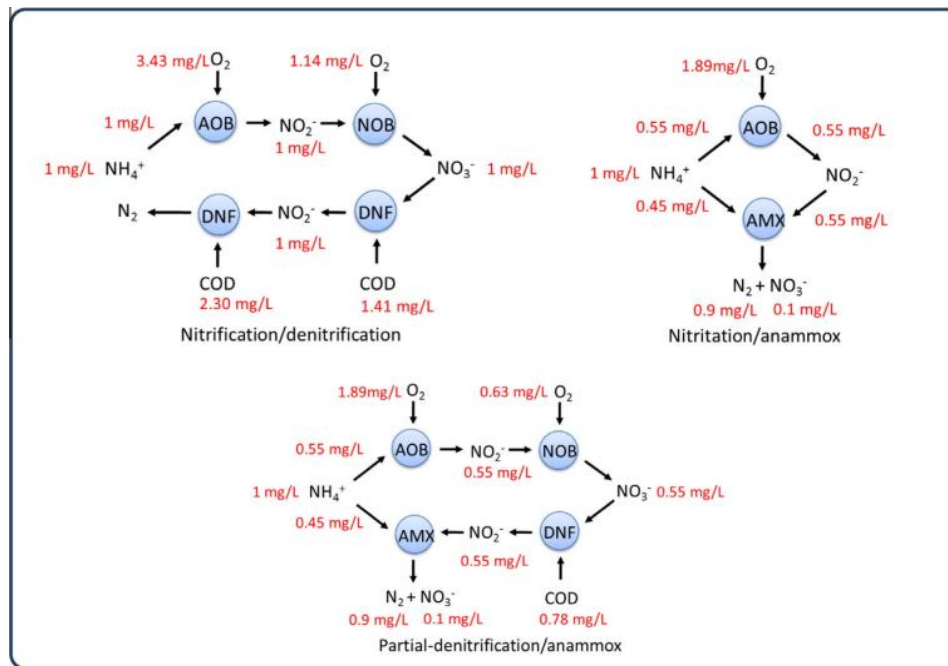
Figure 4-2. Comparison of nitrification/denitrification, nitritation/anammox, and partial-denitrification/anammox processes (Ma et al., 2016)

However, the most common biological process for treating sewage and industrial wastewaters is indeed the activated sludge process. The general arrangement of this process includes two main structures: an aeration tank where air is injected in the mixed liquor, and a clarifier settling tank where biological flocs settle at the bottom of the blanket, thus becoming separate from the clear treated water.

Owing to the presence of multiple biological species, the activated sludge process requires continuous aeration of the mixed liquor to supply these microorganisms with sufficient dissolved oxygen, whereby energy consumption at the aeration tank is very significant. Nevertheless, in addition to its biological role, the forced aeration allows sufficient mixing in the activated sludge tank and contributes to the overall efficiency of the treatment process (Cagdas Ozturk et al., 2016).

Usually, biological process is accepted as the most common and economical method to treat wastewater. However, the activity of microorganisms in the biological treatment systems can be significantly inhibited by high concentrations of ammoniacal nitrogen (NH_3) in swine wastewater (Vadivelu et al., 2007). It is therefore necessary to lower the concentration of ammonia by other ways before executing biological treatments.

4.1.2. Electrochemical treatment

Electrochemical treatment is a separation technology based on the polarity of the dissolved ions. These methods involve a stage of electrolysis. Positive charged ions are attracted by the anode whilst negative ions go to the cathode.

There are different kinds of electrochemical treatments for wastewater. Redox is the most common electrochemical process that entails a direct electrolysis, where oxidation of organic and inorganic compounds from water is produced. Other electrochemical treatments involve an indirect electrolysis, such as electrocoagulation (Guzmán et al., 2016), electroflocculation (Osman et al., 2015), and electroflotation (Aoudj et al., 2015), but are more focused in heavy metal and biomolecule elimination.

Various biochemical and electrochemical methods were investigated and applied for nutrient recovery, in addition to conventional biological treatment. Recently a, a new bioelectrochemical system named "R^2-BES" was developed for removing and recovering nutrients from wastewater (Zhang et al., 2014). Ammonium is removed taking advantage of bioelectricity generation, and present phosphate ions are exchanged by hydroxide ions produced from the cathode reaction. Under an applied voltage of 0.8 V and a current generation of 68.7 mA, ammonium nitrogen was removed by 83.4% and phosphate by 52.4%.

The system consisted of a microbial fuel cell (MFC) with a membrane "pocket" that is responsible of the ionic exchange in the anode and the cathode and that is made of a piece of cation exchange membrane (CEM) and a piece of anion exchange membrane (AEM) (Figure 4-3).

ETSEIB
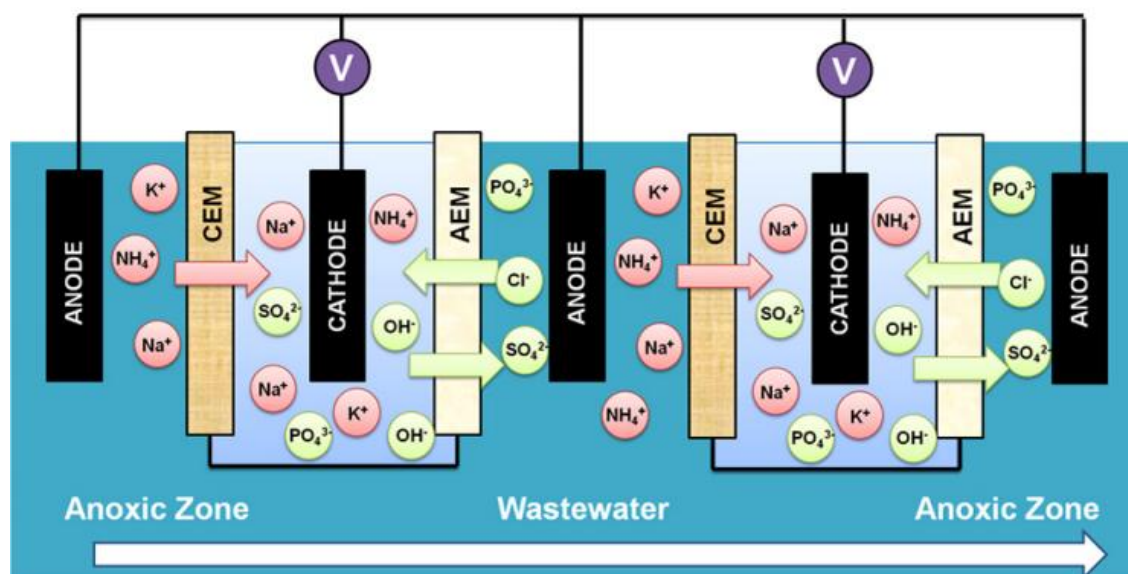
Figure 4-3. R^2-BES electrochemical system

Current density and charge of the water are important facts that affect the effectiveness of electrochemical processes. Presence of NaCl and other salts bumps up the conductivity and hence lowers necessary energy consumption. Anyhow, energy consumption in electrochemical treatments is usually high and becomes one of their big disadvantages, along with its low selectivity for phosphate ions in presence of competing ions (NO_3^-, SO_4^{2-}, HCO_3^-, Cl^-...)

4.1.3. Precipitation

Precipitation consists of adding metallic cations to the wastewater for reacting with the present nutrients forming insoluble or slightly soluble salts that shall precipitate. These salts can be easily separate from the aqueous medium by filtration and be used as the alternative of agricultural fertilizer or as the phosphate rock for phosphate industry. Ferric phosphate ($FePO_4 \cdot 2H_2O$), struvite ($MgNH_4PO_4 \cdot 6H_2O$), calcium phosphates ($Ca(H_2PO_4)_2$), or apatite ($Ca_5(PO_4)_3(F, Cl, OH)$) are very common resulting salts from phosphate precipitation.

Phosphorus removal and recovery by ferric phosphate precipitation using ferric chloride has been considered as an effective technology (Zhang et al., 2010). However, among the alternative processes, struvite (MAP) precipitation has been proven to be a promising method for the removal of ammonia nitrogen as well because of the high reaction rate and removal ratio (Kochany and Lipczynska-Kochany, 2009). Precipitation using magnesium salts

potentially provide simultaneous removal of PO_4^{3-} and NH_4^+ from wastewater. The reaction between Mg^{2+}, PO_4^{3-} and NH_4^+ forms the mineral struvite according to the Equation 4-1 (Warmadewanthi & Liu, 2009):

$$Mg^{2+} + NH_4^+ + PO_4^{3-} + 6H_2O \rightarrow MgNH_4PO_4 \cdot 6H_2O \text{ (struvite)} \qquad \text{Eq. 4-1}$$

Because it is only slightly soluble in water and soil solutions, slow-release struvite has been found to be a highly effective source of phosphorus, nitrogen and magnesium for plants through both foliar and soil application (Li & Zhao, 2003).

There are several chemical combinations to enhance struvite precipitation. Most common are: $MgCl_2 \cdot 6H_2O$ + $Na_2HPO_4 \cdot 12H_2O$, MgO + 85% H_3PO_4 and $MgSO_4 \cdot 7H_2O$ + $Ca(H_2PO_4) \cdot H_2O$ (Li & Zhao, 2003). Results reported that ammonium nitrogen was recovered by 92%, 36% and 70%, respectively, using the designated chemicals, at pH 9.0 and a molar Mg:N:P ratio of 1:1:1. Nevertheless, the effectiveness of MAP precipitation process depends on two main factors: pH value and molar ratio of Mg:N:P. Warmadewanthi & Liu (2009) reported that 47.4% phosphate was removed using magnesium chloride ($MgCl_2 \cdot 6H_2O$) with a stoichiometric ratio of 1:1:1 at pH 9.0, and removal efficiency increased significantly by increasing the Mg:P molar ratio to 3:1, reaching a maximum of 92.1% but with poor ammonium removal efficiency. Bi et al. (2014) performed the same experiment under optimized conditions of Mg:P ratio of 1.8 and pH 9.7, obtaining recovery rates of 46.8% for phosphate and 16.5% for ammonium. According to studies performed by Song et al. (2007), the optimum pH value for MAP crystallization is in the range of 9.5-10.5, although the co-existing of calcium in solution may disturb the morphology and purity of the MAP product, forming amorphous calcium phosphate.

Struvite can be also obtained as the result of the combination of adsorption and precipitation, if the Mg^{2+} released from adsorption processes serves as the magnesium source in struvite crystallization (Figure 4-4). Some experiments of adsorption on modified zeolite in combination with struvite crystallization have been made, where ammonium and phosphate removal efficiency were reported to reach 82% and 98% respectively (Huang, Xiao et al., 2014).

If struvite were to be recovered from wastewater treatment plants worldwide, 0.63 million tons of phosphorus (as P_2O_5) could be harvested annually, reducing phosphate rock mining by 1.6% (Shu et al., 2006).
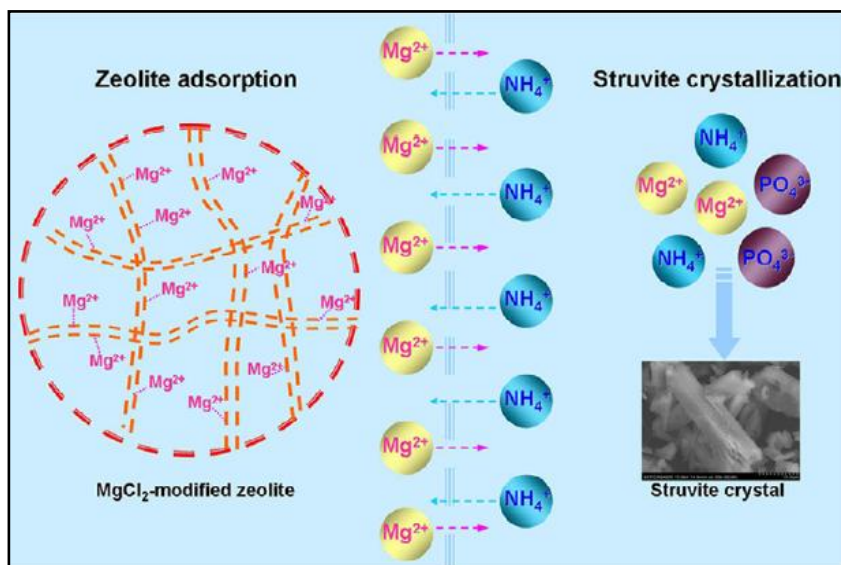
Figure 4-4. Simultaneous removal of NH_4^+ and PO_4^{3-} from swine wastewater by adsorption of modified zeolite combined with struvite crystallization. (Huang, Xiao et al., 2014)

4.1.4. Adsorption

Adsorption processes consist of the adhesion of an adsorbate onto the surface of a sorbent material. Ionic sorption consists of an ionic exchange between the aqueous medium and the surface of a sorbent. It is a widely used technology for its numerous advantages: high efficiency and sustainability, very low energy consumption, flexibility, selectivity, and most important, that sorbents are economic and have a widespread availability.

There are many types of sorbents which have been used for nutrient removal from wastewater and industrial effluents. Activated carbon (Mailler et al, 2016), clay minerals like bentonite (Sun et al., 2015), biomaterials (G. Crini, 2005), natural (S. Wang et al., 2010) and synthetic zeolites (Wu et al., 2007; C. Wang et al., 2009), and some industrial solid wastes such as fly ashes generated from electric power plants (S. Wang et al., 2006)) have been widely used as sorbents for adsorption of ions and organics in wastewater treatment.

Zeolites are becoming most interesting in last decades. Zeolites are crystalline hydrated aluminosilicates with a framework structure of $[SiO_4]^{4-}$ and $[AlO_4]^{5-}$ tetrahedra containing

Nutrient recovery from wastewater by adsorption on Magnesium/Potassium zeolites
in adsorption-ultrafiltration hybrid systems

Page 19

pores occupied by water, alkali and alkaline earth cations (Querol et al., 2002). A wide variety of zeolites can be found in the nature (Table 4-1).

Table 4-1. Some natural zeolites and its structure (S. Wang et al, 2010)

Zeolite	Chemical formula
Clinoptilolite	$(K_2, Na_2, Ca)_3Al_6Si_{30}O_{72} \cdot 21H_2O$
Mordenite	$(Na_2, Ca)_4Al_8Si_{40}O_{96} \cdot 28H_2O$
Chabazite	$(Ca, Na_2, K_2)_2Al_4Si_8O_{24} \cdot 12H_2O$
Phillipsite	$K_2(Ca, Na_2)_2Al_8Si_{10}O_{32} \cdot 12H_2O$
Scolecite	$Ca_4Al_8Si_{12}O_{40} \cdot 12H_2O$
Stilbite	$Na_2Ca_4Al_{10}Si_{26}O_{72} \cdot 30H_2O$
Analcime	$Na_{16}Al_{16}Si_{32}O_{96} \cdot 16H_2O$
Laumontite	$Ca_4Al_8Si_{16}O_{48} \cdot 16H_2O$
Erionite	$(Na_2K_2MgCa_{1.5})_4Al_8Si_{28}O_{72} \cdot 28H_2O$
Ferrierite	$(Na_2, K_2, Ca, Mg)_3Al_6Si_{30}O_{72} \cdot 20H_2O$

The general chemical formula of zeolites is represented in Equation 4-2:

$$M_{x/n}[Al_xSi_yO_{2(x+y)}] \cdot pH_2O \qquad \text{Eq. 4-2}$$

Where *M* is (Na, K, Li) and/or (Ca, Mg, Ba, Sr), and *n* is cation charge; y/x = 1-6, p/x = 1-4.

In spite that natural zeolites are widely used as sorbents because of their effectiveness and natural wealth, synthesized zeolites from coal fly ash have much higher sorption capacities and are gaining importance and value in this field of science and technology. Both natural and synthesized zeolites can be also brought under modifications in order to change their sorption properties, generally achieving better sorption rates for both organic and inorganic nutrients. Modifications can be made in several methods such as acid treatment, ion exchange, and surfactant functionalisation.

4.1.5. Membrane filtration

Membrane technologies have been identified as the most robust and flexible technologies used to improve water quality by removing undesirable compounds and pathogens. Reverse osmosis (RO), nanofiltration (NF), ultrafiltration (UF) and reverse electrodialysis (RED) are being applied worldwide to meet these needs (López-Roldán et. al, 2016).

In most of wastewater treatments, many of these methods are combined in order to enhance separation of desired nutrients from the water, so hybrid membrane processes are being continuously developed as innovating technologies.

Kim et al. (2016) analyzed the performance of a tri-combined desalination process that consists of reverse osmosis (RO), membrane distillation (MD) and pressure-retarded osmosis (PRO). In brief, the recovery rate was 49.7%, i.e., the water production and brine flow rate were 995 m^3/d and 1005 m^3/d, respectively.

Forward osmosis can be effective too, if it is correctly performed. Anammox was combined with forward osmosis in a single process to remove reverse-fluxed ammonium using ammonium bicarbonate as a draw solute, maintaining an effluent ammonium concentration of 3.1 $mg \cdot dm^{-3}$, compared to the concentration of 9.9 $mg \cdot dm^{-3}$ achieved by the sole anammox process (Li et al, 2015).

Another combination of two different processes in a single system was designed for phosphorus recovery (Luo et al., 2016). In this case a reverse osmotic system was joined to an osmotic membrane bioreactor (OMBR), enhancing precipitation of amorphous calcium phosphates with phosphorus content of 15-20% at pH 10. These salts were periodically captured by a MF membrane inside the OMBR, which also controlled salinity build-up in the bioreactor and ensured stable biological performance.

Adsorption/ultrafiltration hybrid systems are gaining importance too in this field of separation technology. Several combinations of sorbents with UF membranes have been implemented, such as for example: a hybrid adsorption/ultrafiltration process for perchlorate removal using chitosan as a sorbent (Xie et al., 2011); the addition of power activated carbon (PAC) adsorption to UF to increase the removal of organic contaminants (Wang et. al, 2016); a wastewater treatment of Palm Oil Mill Effluent (POME) by UF membrane separation coupled with adsorption onto Palm kernel shell - activated carbon (PKS-AC) (Azmi & Yunos, 2014); or novel mixed matrix hollow fiber membranes prepared with super adsorbent carbon nanoparticle and polysulfone, to enhance benzene, phenol and toluene removal from aqueous solution (Mukherjee & De, 2016).

ETSEIB

5. Materials and methods

5.1. Raw materials

Provided Sodium zeolite (NaP1) was synthesized from residual coal fly ash from a coal power plant in Narcea (Asturias, Spain). Synthesis was made through an 8 hours reaction with NaOH 3M at 125 °C, details are provided elsewhere (Querol et al., 2007).

5.2. Preparation of Magnesium/Potassium modified zeolite

Zeolite modification consisted in two steps, firstly a pretreatment and then a salt treatment.

The pretreatment consisted of mixing 30 g of raw zeolite with 250 cm^3 of NaCl 1M, and carrying out a magnetic agitation for 24 hours. After this, a vacuum filtration was done before cleaning the filtered zeolite with deionized water in order to rid possible remaining NaCl solution.

Salt treatment consisted of mixing 30 g of pretreated zeolite with 250 cm^3 of 1M $MgCl_2$-KCl and 1M $MgCl_2$ solutions, for Mg/K-Ze and Mg-Ze, respectively. Stirring was made twice for 4 hours at room temperature (filtrating between one and another) and then a vacuum filtration and a deep cleaning was performed before placing the modified cleaned zeolite into the oven at 50 °C for 72 hours.

5.3. Equilibrium sorption experiments: binary systems

A series of test solutions of 35 cm^3 were prepared with different concentrations of ammonium and phosphate. Concentrations of ammonium ranged from 2 to 4000 mg/dm^3, and phosphate concentrations from 6 to 12000 mg/dm^3.

25 cm^3 of these samples were mixed by a magnetic agitator with 0.1 g of zeolite for 24 hours until equilibrium was achieved. The remaining 10cm^3 were used for analysis. Total ammonium and phosphate concentration was determined by ionic chromatography before and after agitation.

All solutions that contained phosphate were prepared from $NaH_2PO_4 \cdot 2H_2O$ or K_2HPO_4 while ammonium was prepared from NH_4Cl.

Equilibrium sorption capacity of ammonium and phosphate and the removal efficiency (%) were calculated, respectively, from Equations 5-1 and 5-2:

$$q_e = \frac{(C_0 - C_e) \cdot V}{m_{Ze}} \qquad\qquad \text{Eq. 5-1}$$

$$efficiency \ (\%) = \frac{(C_0 - C_e)}{C_0} \cdot 100 \qquad\qquad \text{Eq. 5-2}$$

Where q_e is the sorption capacity at the equilibrium [mg·g^{-1}], C_0 is the initial sorbent concentration [mg·dm^{-3}], C_e is the concentration of the sorbent at the equilibrium [mg·dm^{-3}], V is the batch volume [dm^3] of the sample solution and m_{Ze} is the mass of zeolite [g].

Two conventional isotherm equations were used to describe the sorption process: Langmuir and Freundlich.

5.3.1. Langmuir isotherm

The Langmuir isotherm assumes that adsorption happens at specific homogeneous monolayer sites within the adsorbent, and there is no interaction between the adsorbate molecules. The original form of this model is described by Equation 5-3:

$$\frac{d\theta}{dt} = K_1 PN(1-\theta) - K_{-1}N(1-\theta) \qquad\qquad \text{Eq. 5-3}$$

Where θ is the local surface coverage (concentration of occupied sites by adsorbate), K_1 and K_{-1} are rate constants for adsorption and desorption respectively, P is the pressure above the surface and N is the total number of sites on the surface.

Assuming that $K_L = \frac{K_1}{K_{-1}}$, and applying the model at the equilibrium state of the sorption mechanism of a solid adsorbate, the isotherm can be represented as in Eq. 5-4 (M. Zhang et al., 2011):

$$q_e = \frac{K_L q_m C_e}{1 + K_L C_e} \qquad\qquad \text{Eq. 5-4}$$

Where C_e is the equilibrium concentration [mg·dm^{-3}], q_e is the sorption capacity at the

Nutrient recovery from wastewater by adsorption on Magnesium/Potassium zeolites
in adsorption-ultrafiltration hybrid systems

Page 23

equilibrium [mg·g^{-1}], q_m is the maximum adsorption capacity [mg·g^{-1}], and K_L is the Langmuir constant, which is related to the affinity of the binding sites and energy of adsorption [dm^3/mg].

The linearized form of this model is represented by Eq. 5-5:

$$\frac{C_e}{q_e} = \frac{C_e}{q_m} + \frac{1}{K_L q_m} \qquad \text{Eq. 5-5}$$

Where q_m is the inverse of the slope and $\frac{1}{K_L q_m}$ is the y-intercept of the line.

5.3.2. Freundlich isotherm

The Freundlich isotherm is an empirical equation describing adsorption onto a heterogeneous surface (M. Zhang et al., 2011). It is expressed as in Equations 5-6 or 5-7 (linearized forms):

$$q_e = K_F C_e^{\frac{1}{n}} \qquad \text{Eq. 5-6}$$

$$log\ q_e = log\ K_F + \frac{1}{n} log\ C_e \qquad \text{Eq. 5-7}$$

Where C_e is the equilibrium concentration [mg·dm^{-3}], q_e is the sorption capacity at the equilibrium [mg·g^{-1}], and K_F and n are Freundlich constants related to the adsorption capacity and adsorption intensity of the sorbent, respectively. The n should be in the range of 1-10 for favored adsorption.

5.4. Kinetic studies

In order to perform the kinetic study, a single solution of 250 cm^3 of synthetic water was prepared and mixed with 1 g of zeolite. The concentration of ammonium and phosphate in this solution was respectively 10 and 30 mg/dm^3. Then, the system was brought under magnetic agitation while different samples have been taken every: 2 minutes, during the first 20 minutes; 10 minutes until 1 hour; and 30 minutes until 3 hours. Last samples were taken at 8 hours and at 24 hours to check that equilibrium was reached.

ETSEIB

Kinetic performance of the zeolites is described by the following macroscopic equation models: pseudo-first order model, pseudo-second order model and Elovich model.

5.4.1. Pseudo-first order model

The pseudo-first order model proposed by Lagergren for describing liquid-solid adsorption systems in 1898 is still widely applied today (Tseng et al., 2010). The adsorption kinetics described by pseudo-first-order model is given by Eq. 5-8:

$$\left(\frac{dq_t}{dt}\right) = K_1(q_e - q_t) \qquad \text{Eq. 5-8}$$

This differential equation can be rewritten as its linear form (Eq. 5-9 and 5-10):

$$q_t = q_e(1 - exp(-K_1t)) \qquad \text{Eq. 5-9}$$

$$\log(q_e - q_t) = \log q_e - K_1t \qquad \text{Eq. 5-10}$$

Where q_e and q_t [mg·g^{-1}] are the amounts of adsorbate adsorbed at equilibrium and at any time t, respectively. K_1 is the adsorption rate constant of pseudo-first-order reaction.

5.4.2. Pseudo-second order model

In pseudo-second order model, the rate-limiting step is the surface chemisorption, where the removal from a solution is due to physicochemical interactions between the two phases (Robati, 2013). This model is described by Eq. 5-11 (Ho & McKay, 1999):

$$\left(\frac{dq_t}{dt}\right) = K_2(q_e - q_t)^2 \qquad \text{Eq. 5-11}$$

However, it is usually represented by its linear form, given by Eq. 5-12:

$$\frac{t}{q_t} = \frac{1}{K_2 q_e{}^2} + \frac{t}{q_e} \qquad \text{Eq. 5-12}$$

Where q_e is the amount of adsorbate adsorbed at equilibrium [mg·g^{-1}] and K_2 is the adsorption rate constant for second-order [mg·g^{-1}·min^{-1}].

5.4.3. Elovich

The Elovich equation, originally presented in 1939, is satisfied in chemical adsorption processes and is suitable for systems with heterogeneous adsorbing surfaces (Feng-Chin Wu

ETSEIB

Nutrient recovery from wastewater by adsorption on Magnesium/Potassium zeolites
in adsorption-ultrafiltration hybrid systems
Page 25

et al., 2009). This equation is one of the most useful models for describing such activated chemical adsorption and is given by Eq. 5-13:

$$\left(\frac{dq_t}{dt}\right) = \alpha\, exp(-\beta q_t) \qquad \text{Eq. 5-13}$$

After integration and linearization, the equation can be expressed as (Inyang et al., 2015):

$$q_t = \frac{1}{\beta}\ln(\alpha\beta) + \frac{1}{\beta}\ln(t) \qquad \text{Eq. 5-14}$$

Where α is the initial sorption rate [mg·g^{-1}·min^{-1}] and β is the desorption constant [mg·g^{-1}] during any experiment (Idris et al., 2011).

5.5. Solid/liquid ratio evaluation experiments

The amount of zeolite was evaluated in order to determine the most suitable solid/liquid ratio for the performance of hybrid UF-sorption pilot plant test. The aim of these studies was to evaluate the effectiveness of the zeolite dose and to find an optimum solid/liquid ratio according to two main criteria: removal efficiency (%) and adsorption capacity. Many samples of 25 cm^3 of wastewater and synthetic water were mixed with different quantities of zeolite for 24 hours. Solid/liquid ratios were ranged from 4 to 80 g Mg-Ze/dm^3.

Notwithstanding, these experiments were carried out to optimize the efficiency of the later experiment at the UF pilot plant (subsection 5.6), and the system does actually not endure higher S/L ratios (larger than 2.5 g/L) due to the fact that the UF-membrane working conditions (intermembrane threshold pressure) do not allow large amounts of solids.

For that reason, dose studies were carried out with lower S/L ratios, ranging from 1.0 to 2.4 g Mg-Ze/dm^3

A total of 16 samples of 150 cm^3 have been analyzed; 8 corresponding to synthetic water samples and 8 to the wastewater samples. Initial concentrations of ammonium and phosphate and S/L ratios are detailed in Tables 5-1 and 5-2.

Table 5-1. NH_4^+ and PO_4^{3-} initial concentrations of wastewater and synthetic water samples

	NH_4^+ [mg/dm^3]	PO_4^{3-} [mg/dm^3]
Wastewater	878.4	31.6
Synthetic water	825.6	107.5

Table 5-2. S/L ratios and total mass of Mg-Ze used for the 150 cm^3 samples

S/L ratio [g/dm^3]	1.0	1.2	1.4	1.6	1.8	2.0	2.2	2.4
Mass [g]	0.15	0.18	0.21	0.24	0.27	0.30	0.33	0.36

In all cases, treated water samples have been analyzed by ionic chromatography before and after the sorption of ammonium and phosphate on zeolites.

5.6. Nutrients recovery in hybrid UF-adsorption pilot plant

Adsorption onto zeolite was combined with ultrafiltration (UF) in a single hybrid system in order to remove ammonium and phosphate simultaneously from wastewater as an effective separation method to separate the zeolite from the treated water.

A pilot plant at laboratory scale (Figure 5-1) was designed in previous works to test a real application of this recovery method, and it was used in this project to perform the nutrients recovery in a continuous reactor.

5.6.1. System and experiment description

The experiment was performed feeding the UF membrane by the stream leaving the stirred tank reactor (STR) that contained a mix of a real 40 dm^3 wastewater sample and magnesium modified zeolite (Mg-Ze). Optimum zeolite dose was added to the reactor and stirring was made for 30 minutes before starting the system to ensure that sorption equilibrium was reached. This solution was forced to enter into the membrane, enhancing the ultrafiltration and separating the loaded zeolite from the water, and obtaining two streams: permeate and concentrate. Permeate was collected into another tank while concentrate was fully recirculated to the STR. A toilet buoy was used to control the flow of the inlet stream from the reserve tank, in order to maintain the STR level constant at 32.5 cm (40 dm^3).
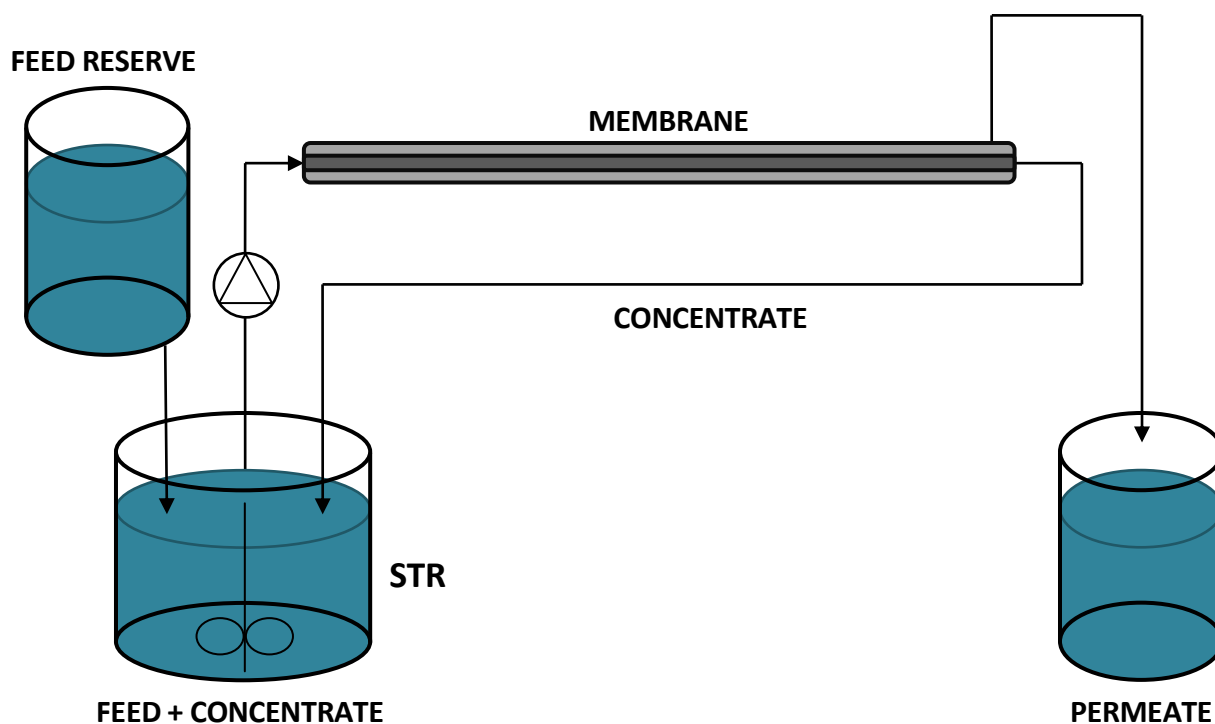
Nutrient recovery from wastewater by adsorption on Magnesium/Potassium zeolites
in adsorption-ultrafiltration hybrid systems
Page 27

FEED RESERVE

MEMBRANE

CONCENTRATE

STR

FEED + CONCENTRATE

PERMEATE

Figure 5-1. Sketch of the UF-adsorption pilot plant

Since the membrane is susceptible to become fouled by the zeolite particles, transmembrane pressure was permanently controlled, and the experiment was divided in cycles as the membrane nedded a countercurrent mechanical cleaning once the maximum threshold pressure (0.85 bar) was achieved. Cleaning was performed by using the permeate, and recovered zeolite from the membrane was returned to the feed tank. Working conditions are detailed in Table 5-3.

Table 5-3. UF membrane specifications and work conditions of the system

Membrane pore size (µm)	0.02
Module length (mm)	1000
Membrane surface (m^2)	0.251
Water permeability (dm^3/hm^{2}bar)	200 to 400
Trans-membrane pressure (bar)	0.25 to 0.85
Feed deposit level (dm^3)	37.5 to 40.0
Zeolite S/L ratio (g/dm^3)	2
Zeolite mass (g)	80
pH feed	8.0 to 8.5
Temperature (ºC)	25
Stirring velocity (rpm)	350 - 400

ETSEIB

5.6.2. Water sample preparation

Since real wastewater had a lot of suspended solids and might saturate the UF-membrane, 80 liters of synthetic water were used instead, thus, preserving the life of the membrane. In order to prepare the synthetic water as most similar to a real wastewater sample as possible, it was necessary to use tap water and then adding the appropriate amounts of salts to reach desired concentrations.

For that reason, tap water was previously analyzed by ionic chromatography to determine the concentration of present cations (Na^+, K^+, Mg^{2+}, Ca^{2+}, NH_4^+) and most of present anions (F^-, Cl^-, NO_3^-, PO_4^{3-}, SO_4^{2-}), and an acid-base titration was carried out to determine hydrogencarbonates (HCO_3^-). With these data, a mass balance was performed to determine the corresponding amounts of salts needed (most of them chlorides and hydrogencarbonates).

5.6.3. Hybrid UF-sorption pilot plant: procedure description

Once the water was prepared, 80 g of zeolite were added to the reactor tank under continuous stirring for 30 minutes until equilibrium was achieved. Meanwhile, samples were taken at 3, 6, 10, 20 and 30 minutes of agitation.

After setting up the pump, the tubes, and the valves, the whole pilot plant was started up and the mixture of water and zeolite began to feed the system. Samples were taken from the STR feed solution and from the permeate stream at 5 minutes and then every 10 minutes, until one cycle was completed. After stopping the system and cleaning the membrane, a new cycle was performed and once again the whole procedure was repeated over and over until the feed reserve tank remained empty.

Pressure was also measured after each sampling procedure as well as the height of the level of the STR and the permeate flow, which is equal to the flow of the entrance from the reserve tank, according to the global balance of the system.

5.6.4. Mass Balance

All calculations done before reporting the results of this study are based on the following mass balance (Galera, 2015):

The mass of X (X = NH_4^+, PO_4^{3-}) adsorbed onto the zeolite, $m(X)_{Ze}$ [mgX-Ze/dm^3] could be calculated by Eq. 5-15:

$$m(X)_{Ze} = m(X)_0 + m(X)_S - m(X)_P - m(X)_T \qquad \text{Eq. 5-15}$$

Where:

$m(X)_0$ [mg] is the initial mass of X introduced in the STR of 40 dm^3 (V) at time zero calculated by Eq. 5-16:

$$m(X)_0 = V * C_0 \qquad \text{Eq. 5-16}$$

$m(X)_S$ [mg] is the mass of X fed from the reserve tank (S) to the reactor for a given filtration time interval ($\Delta t = t_j - t_i$), calculated by Eq. 5-17:

$$m(X)_S = Q_S(t) * \Delta t * \frac{C_{S(i)} + C_{S(j)}}{2} \qquad \text{Eq. 5-17}$$

$m(X)_P$ [mg] is the mass of X leaving the system through the permeate stream (P) for a given filtration time interval, according to Eq. 5-18:

$$m(X)_P = Q_P(t) * \Delta t * \frac{C_{P(i)} + C_{P(j)}}{2} \qquad \text{Eq. 5-18}$$

$m(X)_T$ [mg] is the mass of X at the STR for a given filtration time interval, calculated by Eq. 5-19:

$$m(X)_T = V_T * \frac{C_{T(i)} + C_{T(j)}}{2} \qquad \text{Eq. 5-19}$$

$C_{(i)}$ and $C_{(j)}$ [mgX-Ze/dm^3] are the X concentrations in a given stream of reactor volume at time i and j respectively.

On the other hand, the performance of the hybrid membrane UF-sorption system was evaluated by estimating:

X sorption onto zeolite at a given time instant, $Q_{X(t)}$ [mg X/g Ze] by Eq. 5-20:

ETSEIB

$$Q_{X(t)} = \frac{m(X)_{Ze}}{V_t * g_{Ze}}$$ Eq. 5-20

X removal efficiency ($R_P - X\,(\%)$) by Eq. 5-21:

$$R_P - X(\%) = \left(1 - \frac{C_{P(t)}}{C_{S(t)}}\right) \times 100$$ Eq. 5-21

Where $C_{s(t)}$ and $C_{p(t)}$ are *X* concentrations in reserve feed and permeate streams, respectively, at a given time t.

5.7. Characterization of zeolites

Virgin Mg/K-Ze and Mg-Ze as well as loaded zeolites with the highest concentration binary solution were washed with ultrapure water and were dried in the oven at 60 ºC for physicochemical characterization. Scanning Electron Microscopy (SEM) and Energy Dispersive X-Ray Spectrometry (EDS) technologies were used to analyze the zeolite samples morphology as well as their chemical composition, respectively.

5.8. Sample analysis

5.8.1. Ionic Chromatography

All synthetic water and wastewater samples were analyzed by ionic chromatography (Dionex ICS-1000). This technique allows the separation of different ions according to their retention time in an ionic exchange column. Present analytes interact with the stationary phase of the column and last different time periods in getting across it, depending on their charge and their affinity with the column resin. Once separated, ion concentrations are determined over time by a detector that measures their conductance.

Figure 5-2 is an image of the chromatograph used during this project.

Nutrient recovery from wastewater by adsorption on Magnesium/Potassium zeolites
in adsorption-ultrafiltration hybrid systems
Page 31

Figure 5-2. Dionex ICS-1000 Ionic Chromatography System

5.8.2. SEM/EDS

In regard to solid samples, two different technologies have been used for their chemical and physical characterization: Energy Dispersive X-Ray Spectroscopy (EDS) and Scanning Electron Microscopy (SEM).

EDS was used to obtain the chemical composition of both virgin and loaded zeolite samples. This technique relies on the interaction of an X-ray beam and the sample. Electrons of the focused sample may become excited and ejected to a higher-energy shell, releasing energy in the form of X-rays that are detected by the spectrometer. This energy is characteristic of each element and its atomic structure, so elemental composition of the sample can be measured.

SEM produces images by scanning a sample with a focused beam of accelerated electrons. The focused surface emits back excited electrons that are detected by the microscope. Thus, the topography of a surface is displayed as an image. This technique was used to obtain enlarged images of the morphology of zeolite samples. Figure 5-3 is an image of the equipment used in this project to perform SEM and EDS tests for zeolite characterization.
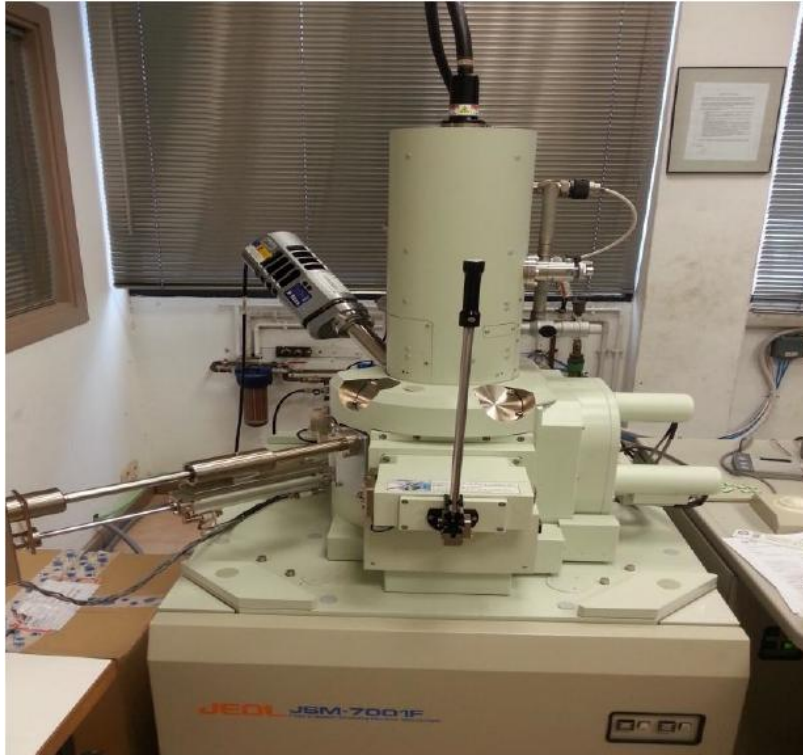
ETSEIB

Figure 5-3. Integrated SEM/EDS module

5.8.3. Total Suspended Solids (TSS)

Wastewater samples used on zeolite dose studies contained such a big amount of suspended solids, fact that made them difficult to analyze and to work with. Total suspended solids factor (TSS) was determined as the follows:

10 cm^3 of wastewater samples were pipetted into a beaker and it was weighted on a balance. Then it was placed in the oven at 50ºC and let for 24 hours in order the water to evaporate completely. Finally, the beaker was weighted again and TSS factor was obtained by mass difference.

ETSEIB

6. Results and discussion

6.1. Characterization of modified zeolites

SEM technology was used to obtain information about the morphology and composition of the Magnesium zeolite and the Potassium/Magnesium zeolite so for both virgin and loaded samples. Images can be observed in Figure 6-1.
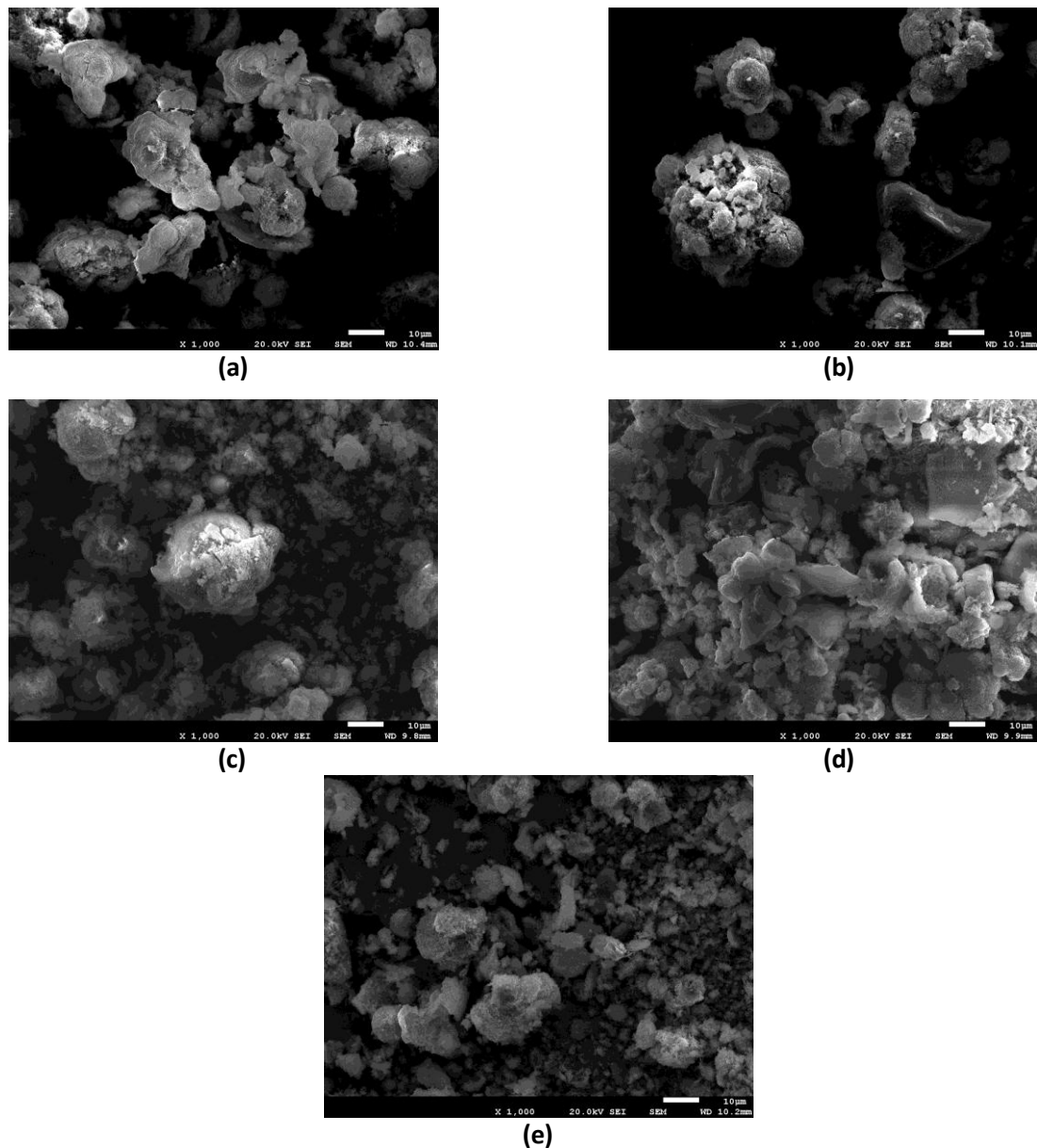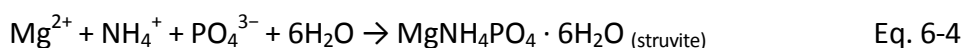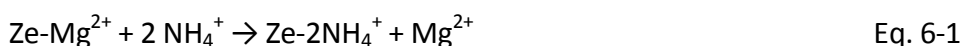

Figure 6-1. SEM images of a) Virgin Mg/K-Ze, b) Virgin Mg-Ze, c) Loaded Mg/K-Ze after sorption experiments with synthetic water, d) Loaded Mg-Ze after sorption experiments with synthetic water, e) Loaded Mg-Ze after sorption experiments with wastewater

As it can be observed, raw zeolites have wider gap zones and are more porous. However, in zeolites that are loaded after sorption experiments, with both synthetic and wastewater, gaps are filled by sorbed particles and structures are more compacted.

The nutrient removal and recovery mechanism consisted of a combination of ionic exchange and struvite precipitation. In the case of Mg/K-Ze, Mg^{2+} and K^+ present on the surface of the zeolite were exchanged by NH_4^+ (Eq. 6-1 and Eq. 6-2), and released Mg^{2+} was the magnesium source for struvite crystallization (Eq. 6-4). Sorption onto Mg-Ze took place in the same way, with the difference that the present ion that was exchanged by NH_4^+ was Na^+ instead of K^+ (in addition to Mg^{2+}) (Eq. 6-3).

$$Ze\text{-}Mg^{2+} + 2\ NH_4^+ \rightarrow Ze\text{-}2NH_4^+ + Mg^{2+} \qquad\qquad \text{Eq. 6-1}$$

$$Ze\text{-}K^+ + NH_4^+ \rightarrow Ze\text{-}NH_4^+ + K^+ \qquad\qquad \text{Eq. 6-2}$$

$$Ze\text{-}Na^+ + NH_4^+ \rightarrow Ze\text{-}NH_4^+ + Na^+ \qquad\qquad \text{Eq. 6-3}$$

$$Mg^{2+} + NH_4^+ + PO_4^{3-} + 6H_2O \rightarrow MgNH_4PO_4 \cdot 6H_2O_{\ (struvite)} \qquad\qquad \text{Eq. 6-4}$$

Loaded samples (c) and (d) seem to contain crystals, which could be precipitated struvite. It is better perceived in sample (d) (see the upper-right part of the image). Sample (e), however, despite of seeming to contain precipitated struvite too, apparently did not fulfill the expectations and was able to recover much less nutrients (empty gaps are wider). This might occur due to the fact that the wastewater contained lots of suspended solids that may disturb nutrients recovery efficiency. Total suspended solids ratio (TSS) of the wastewater was reported to be of 2.5 g/L, which is a significant amount in comparison to synthetic water samples that were prepared with ultrapure water.

EDS analysis provided information about the chemical composition of both virgin and loaded zeolites, in terms of mass (%). This additional information helped to observe how efficient the modification process of each zeolite was, and also to explain their sorption performance. The EDS analysis report for each zeolite is summarized in Table 6-1.

Both Mg-Ze and Mg/K-Ze samples reported overall a very little composition of phosphorus, but it was enough to perceive that struvite was slightly adsorbed. Removed PO_4^{3-} might be precipitated as struvite but not sorbed onto the zeolite surface completely, apparently, only

a small amount.

Table 6-1. Chemical composition (wt %) of salt modified zeolites

Element	Virgin NaP1[1]	Virgin Mg/K-Ze (a)	Virgin Mg-Ze (b)	Loaded Mg/K-Ze (c)	Loaded Mg-Ze (d)	Loaded Mg-Ze (e)
O	51.3	53.95	59.21	57.34	53.54	58.26
Na	8.4	-	5.74	-	0.77	-
Mg	0.7	1.44	1.84	3.51	2.49	0.59
Al	9.6	10.02	9.92	7.40	11.38	10.62
Si	17.9	18.69	18.72	15.48	21.62	18.74
P	-	-	-	0.26	0.72	2.61
K	2.2	11.32	-	2.24	1.25	5.54
Ca	1.5	1.30	2.02	5.75	3.45	0.51
Ti	-	0.46	-	0.53	-	-
Mn	-	-	-	0.38	-	-
Fe	2.7	2.81	2.55	7.11	4.77	3.13

It can be observed that during the modification, a successful exchange between K^+ and Na^+ occurred for Ze-Mg/K zeolite. However, Mg^{2+} was not fully exchanged during the modification, due to lack of affinity. According to results reported by Widiastuti et al. (2011), Magnesium is the cation that has less affinity towards zeolite surface: **$K^+ > NH_4^+ > Na^+ > Ca^{2+}$ $> Fe^{3+} > Al^{3+} > Mg^{2+}$**. The same occurred in the modification to Ze-Mg, where the zeolite remained mainly composed by sodium, and only a few part of the existing Na^+ was exchanged by Mg^{2+}.

Therefore, it is comprehensible and expected that magnesium zeolite has a high sorption capacity for ammonium, but low capacity for phosphate, as it is reported later in subsection 6.2.

---

[1] (Qiu, 2015)

6.2. Ammonium and phosphate sorption capacity

In Figures 6-2 and 6-3, the experimental data of the equilibrium sorption on Mg/K-Ze are represented as well as the theoretical Langmuir and Freundlich isotherm prediction for ammonium and phosphate in a NH_4^+/PO_4^{3-} binary system.
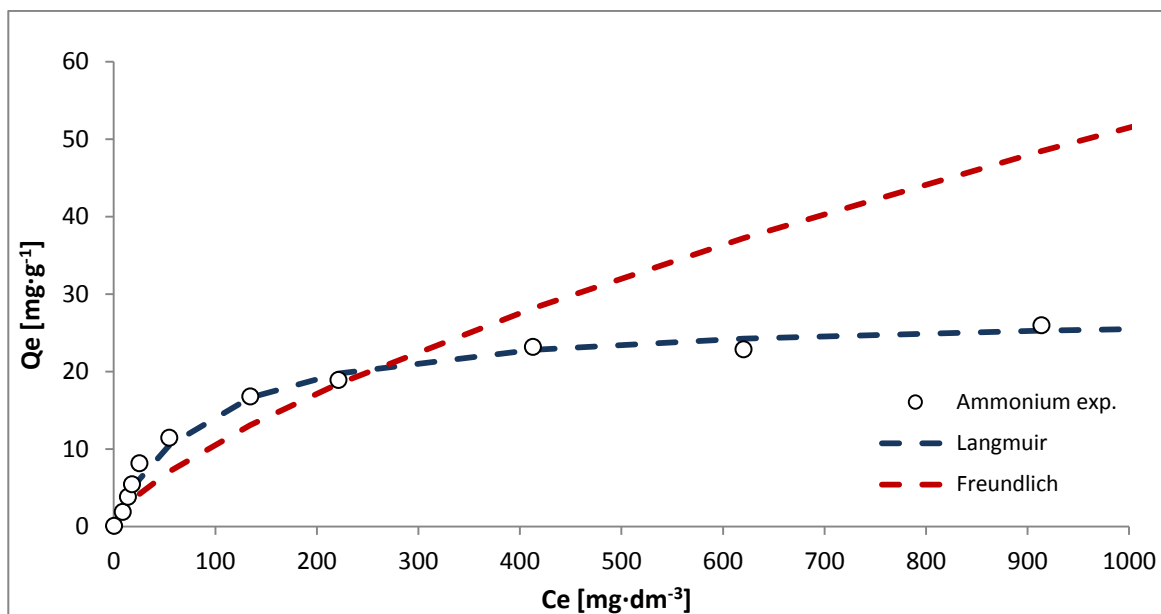

Figure 6-2. Experimental and isotherm prediction by Langmuir and Freundlich equations for ammonium adsorption onto Mg/K-Ze
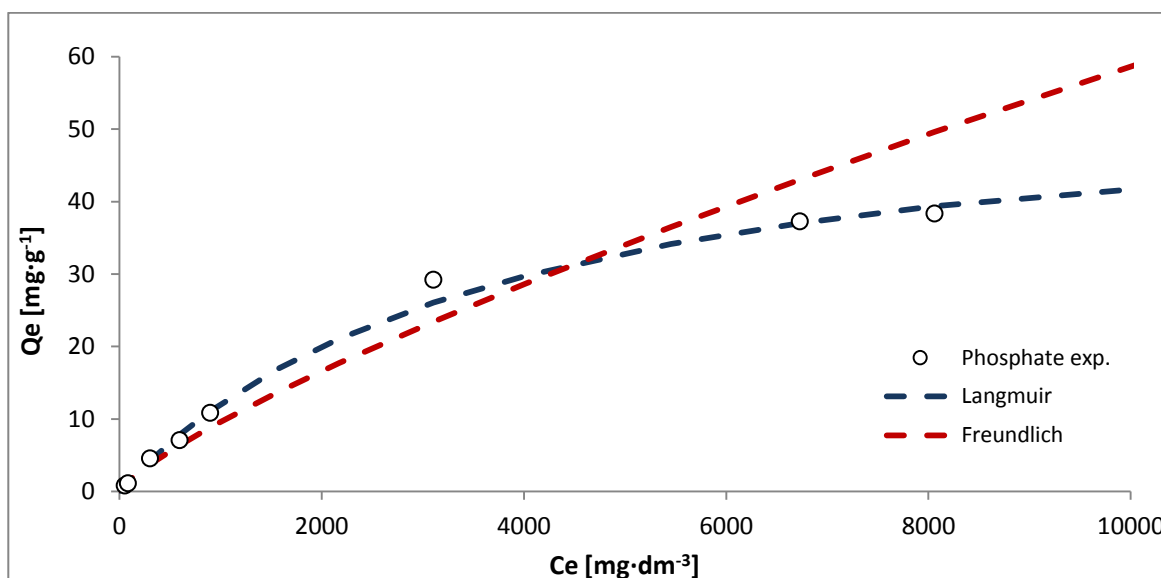

Figure 6-3. Experimental and isotherm prediction by Langmuir and Freundlich equations for phosphate adsorption onto Mg/K-Ze

Nutrient recovery from wastewater by adsorption on Magnesium/Potassium zeolites
in adsorption-ultrafiltration hybrid systems
Page 37

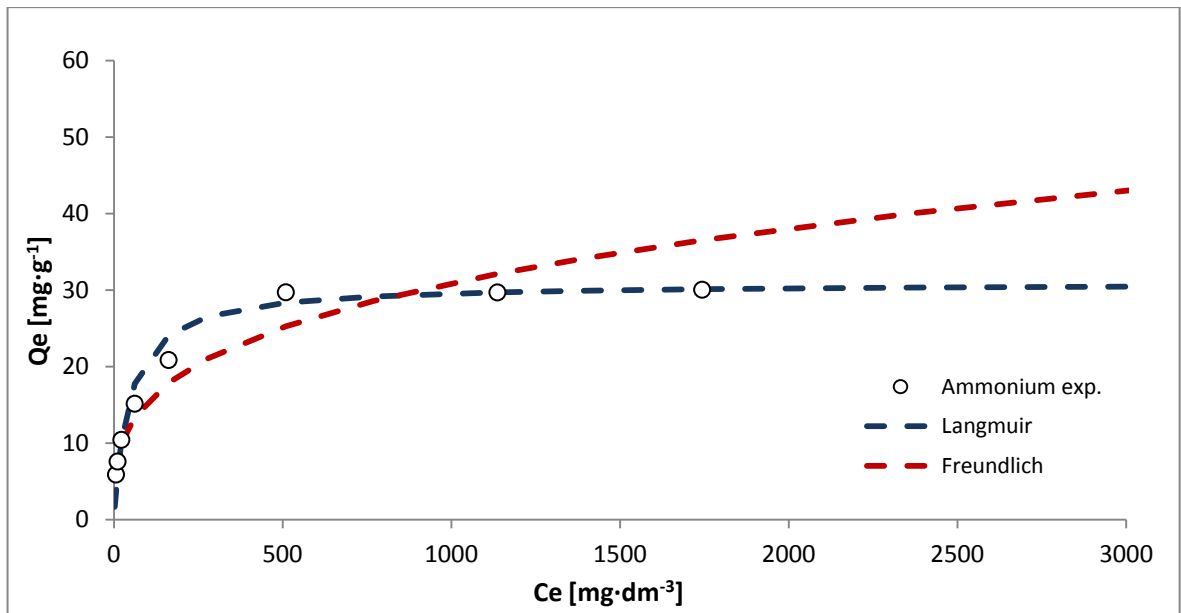The Mg-Ze performance for ammonium and phosphate is shown in Figures 6-4 and 6-5, respectively.

Figure 6-4. Experimental and isotherm prediction by Langmuir and Freundlich equations for ammonium adsorption onto Mg-Ze (binary system)
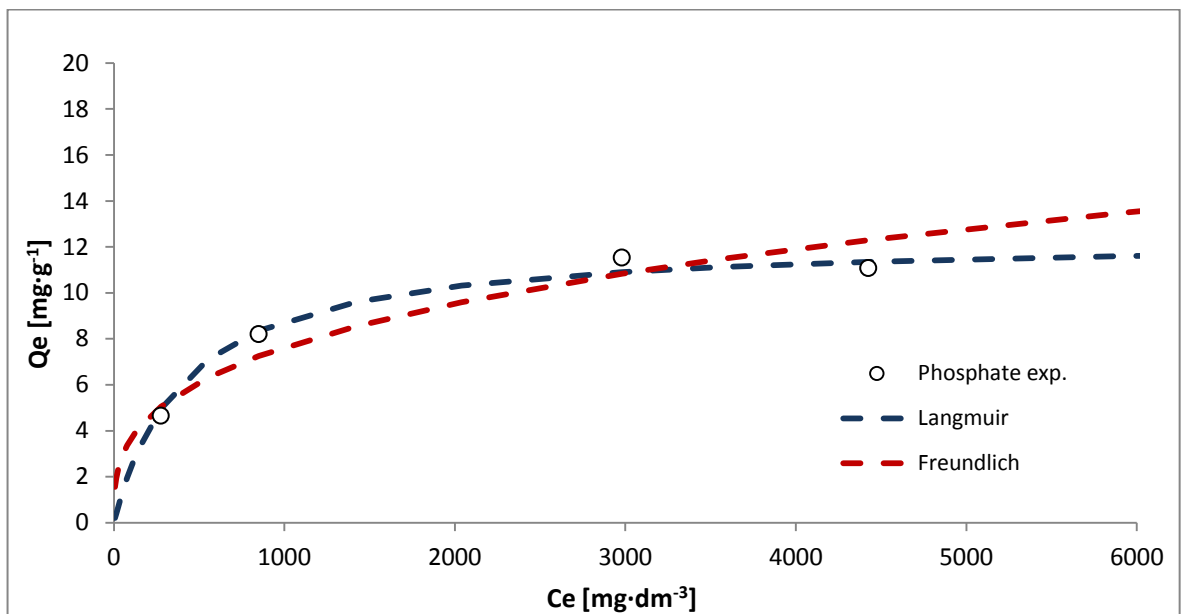

Figure 6-5. Experimental and isotherm prediction by Langmuir and Freundlich equations for phosphate adsorption onto Mg-Ze (binary system)

The sorption parameters for both zeolites are collected in Table 6-2. Mg-Ze has a higher sorption capacity for ammonium than the Mg/K-Ze form, even that are in the same order of magnitude. On the contrary, Mg/K-Ze has a better sorption capacity for phosphate than Mg-Ze. Mg/K-Ze has a maximum phosphate sorption capacity of 58 mg·g^{-1}, while Mg-Ze sorbs up to 12 mg·g^{-1}. However, the sorption parameters for Mg-Ze performance in this study do not concur with the ones that were reported for the same zeolite in previous thesis. This occurs due to some changes made in this project at the modification method, which make these variances comprehensible. One of these changes is the lack of heating during the magnetic stirring. In previous projects, NaP1 modification to other forms was made by stirring at 50 ºC, which endows Mg^{2+} ions of energy to diffuse into the zeolite. At 20 ºC though, diffusion becomes slower and less effective.

As it is shown in Table 6-2, all the equilibrium sorption experiments that have been done fit the Langmuir equation model.

Table 6-2. Isotherm parameters for adsorption of NH_4^+ and PO_4^{3-} onto different zeolites

		LANGMUIR			FREUNDLICH		
		R^2	K_L	q_m	R^2	K_F	n
Mg/K-Ze	Ammonium	0.99	$1.1 \cdot 10^{-2}$	27.8	0.91	$4.6 \cdot 10^{-1}$	1.5
	Phosphate	0.98	$2.6 \cdot 10^{-4}$	57.9	0.98	$4.2 \cdot 10^{-2}$	1.3
Mg-Ze	Ammonium	0.99	$2.2 \cdot 10^{-2}$	30.9	0.95	3.9	3.3
	Phosphate	0.99	$2.4 \cdot 10^{-3}$	12.4	0.93	$8.4 \cdot 10^{-2}$	3.1

In Table 6-3 it can be observed that zeolites studied in the present project are competitive with other natural and synthetic zeolites the performance of which was formerly reported by different researchers. Sorption capacities for ammonium and phosphate as well as the characteristic functional ions are compared.

Table 6-3. Comparison between sorption capacities of different natural and synthetic zeolites

Zeolite	Active ion	$Q_m(NH_4^+)$ [mg·g^{-1}]	$Q_m(PO_4^{3-})$ [mg·g^{-1}]	Comment	Reference
Na-ZFA	Na^+	<20 %$_{RE}$ *	35.31	$Q_m(PO_4^{3-})$ Represented in mgP·g^{-1} using C_0=1000 mgP·dm^{-3}	Wu et al. (2006)
Ca-ZFA	Ca^{2+}	40-54 %$_{RE}$ *	54.17	$Q_m(PO_4^{3-})$ Represented in mgP·g^{-1} using C_0=1000 mgP·dm^{-3}	Wu et al. (2006)
Mg-ZFA	Mg^{2+}	43-58 %$_{RE}$ *	32.79	$Q_m(PO_4^{3-})$ Represented in mgP·g^{-1} using C_0=1000 mgP·dm^{-3}	Wu et al. (2006)
Fe-ZFA	Fe^{3+}	<1 %$_{RE}$ *	31.75	$Q_m(PO_4^{3-})$ Represented in mgP·g^{-1} using C_0=1000 mgP·dm^{-3}	Wu et al. (2006)
Al-ZFA	Al^{3+}	80-98 %$_{RE}$ *	30.46	$Q_m(PO_4^{3-})$ Represented in mgP·g^{-1} using C_0=1000 mgP·dm^{-3}	Wu et al. (2006)
LC-Z/HC-Z	Ca^{2+}	42-60 %$_{RE}$ *	74-98 %$_{RE}$ *	Synthesized zeolites from low-calcium (LC-Z) and high calcium (HC-Z) fly ashes	Ji et al. (2015)
Mg-Ze	Mg^{2+}	30.9	12.4		This work
Mg/K-Ze	Mg^{2+}, K^+	27.8	57.9		This work
New Zealand clinoptilolite	Na^+, K^+, Ca^{2+}, Mg^{2+}	8.5	n.a.		Weatherley et al. (2004)
New Zealand mordenite	Na^+, K^+, Ca^{2+}, Mg^{2+}	12.2	n.a.		Weatherley et al. (2004)
Croatian clinoptilolite	Na^+, K^+, Ca^{2+}, Mg^{2+}	13.6	n.a.		Rozic et al. (2000)
Chinese clinoptilolite	Na^+, K^+, Ca^{2+}, Mg^{2+}	11.2	n.a.		Wang et al. (2007)
Turkish clinoptilolite	Na^+, K^+, Ca^{2+}, Mg^{2+}	5.7 - 7.7	n.a.	At 30 °C temperature	Karadag et al. (2007)
Canadian clinoptilolite	Na^+, K^+, Ca^{2+}, Mg^{2+}	18.5 - 22.9	n.a.	At 20 °C temperature	Liu et al. (2001)
USA clinoptilolite	Na^+, K^+, Ca^{2+}, Mg^{2+}	18.5	n.a.	At 20-21 °C temperature	Guo et al. (2007)
Iranian clinoptilolite	Na^+, K^+, Ca^{2+}, Mg^{2+}	17.8	n.a.	At 28 °C temperature	Ashrafizadeh et. al (2008)

* %$_{RE}$ ≡ removal efficiency (%)

6.3. Kinetic performance of the zeolites

Even though adsorption kinetics are quick and all important changes can be observed within the first three hours of agitation, stirring was made for 24 hours to assure that equilibrium was achieved.

Kinetic studies were carried out following the procedure described in section 5.4 and reported results for phosphate and ammonium sorption into Ze-Mg/K kinetics are represented in Figure 6-6.
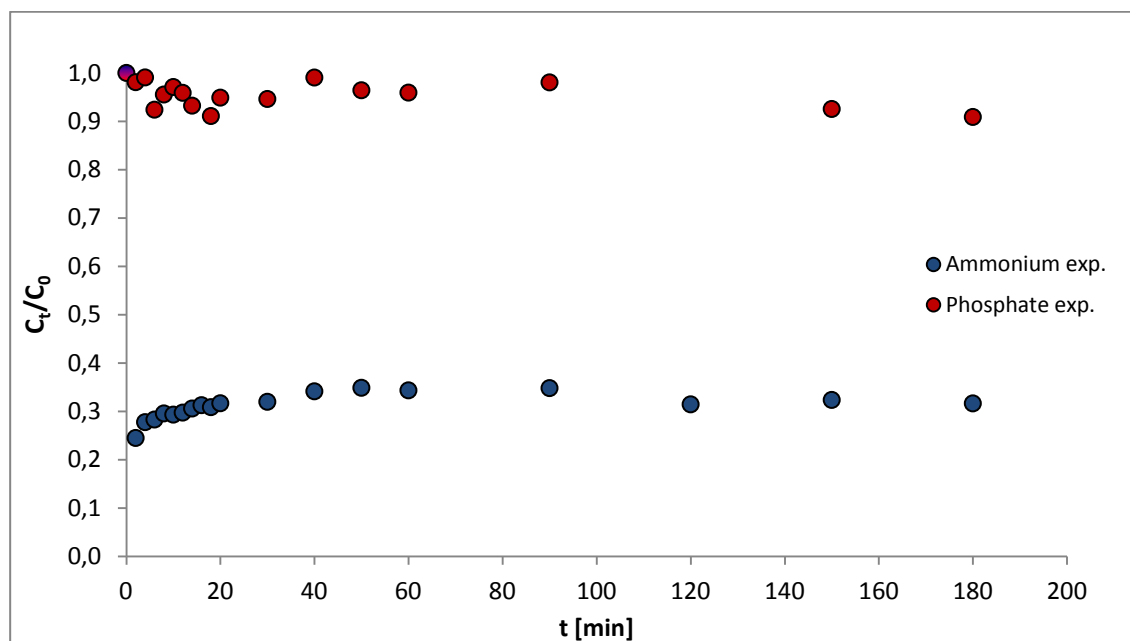

Figure 6-6. Kinetic performance of Mg/K-Ze on NH_4^+ and PO_4^{3-} sorption

As shown in Figure 6-6, ammonium sorption was extremely quick since ammonium ions have much more affinity toward the sorbent than sodium and magnesium ions, and the first noticeable equilibrium was reached after 2 minutes of agitation. From then on, ions looked forward for a more stable equilibrium. On the contrary, phosphate sorption was slow and long-termed through the first 3 hours.

In addition, it is worth to mention that phosphate recovered was less than 10% while ammonium recovery efficiency was close to 70%. This was expected since Mg^{2+} required for struvite crystallization was not successfully exchanged during the modification to Mg/K-Ze, as explained previously in subsection 6.1

Nutrient recovery from wastewater by adsorption on Magnesium/Potassium zeolites
in adsorption-ultrafiltration hybrid systems

Page 41

Kinetic parameters of the models presented in subsection 5.4 were determined by fitting the experimental results and are detailed in Table 6-4. Results show that the Mg/K-Ze kinetic performance fit well with the pseudo-second order model.

Table 6-4. Isotherm parameters for adsorption of NH_4^+ and PO_4^{3-} onto different zeolites

			Mg/K-Ze synthetic water	
			Ammonium	**Phosphate**
Pseudo 1st order	R^2		$1.00 \cdot 10^{-3}$	0.79
	q_e		0.3	0.4
	K_1		$-2.8 \cdot 10^{-7}$	$1.6 \cdot 10^{-4}$
Pseudo 2nd order	R^2		0.99	0.97
	q_e		2.6	0.6
	K_1		$2.5 \cdot 10^{-3}$	$1.5 \cdot 10^{-3}$
Elovich	R^2		0.49	0.90
	α		$-3.56 \cdot 10^{-27}$	0.16

As the Mg-Ze form was selected to be used in the work at the UF-adsorption pilot plant (subsection 6.5), the kinetic performance of this zeolite was studied through batch experiments with real wastewater samples, but due to the complexity of the water composition, the kinetic performance was not able to be fitted by any of the three kinetic models proposed (pseudo-first, pseudo-second and Elovich models). The experimental data are represented in Figure 6-7.
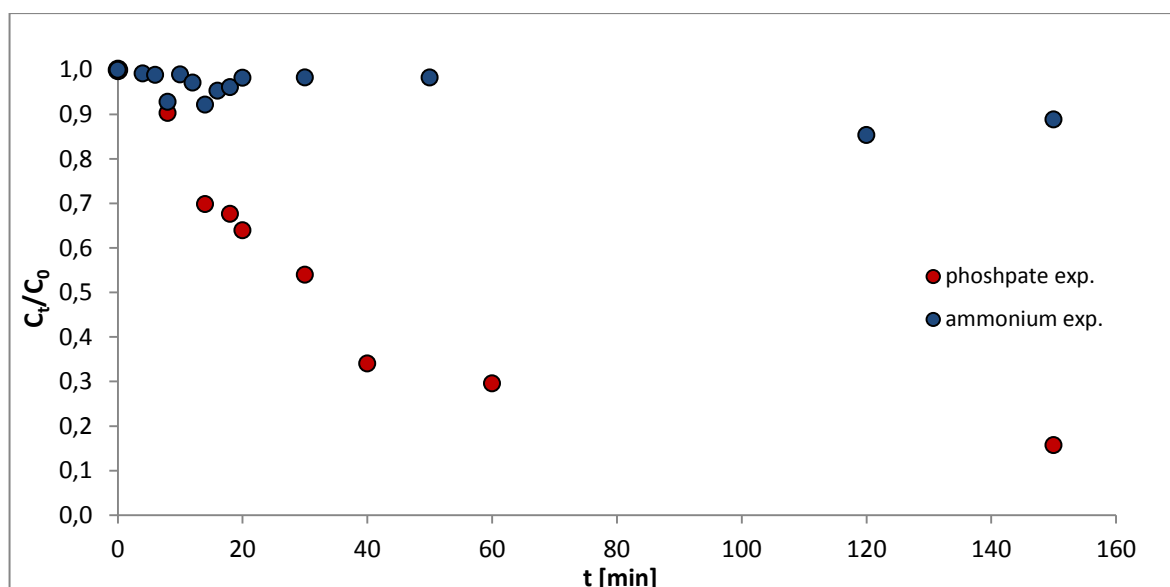

Figure 6-7. Kinetic performance of Mg-Ze on NH_4^+ and PO_4^{3-} sorption

In this case, ammonium recovery was poor, achieving less than 15% after 3 hours. Phosphate, on the contrary, was recovered almost on its totality. This was expected, since Mg^{2+} was successfully exchanged during the modification process (subsection 6.1), and thus was able to trigger struvite crystallization.

6.4. Solid/liquid ratio evaluation experiments

In order to select the solid/liquid ratio to be used in the hybrid pilot plant, an equilibrium dose study using wastewater was carried out using different quantities of Magnesium zeolite for each sample of 25 cm^3. The Mg-Ze form was selected because its sorption capacity and also due to the phosphate was preferred to be obtained as struvite, since it is easier to recover. Therefore, it was needed a zeolite with higher magnesium content as active ion, while the Mg/K-Ze form was mainly composed by potassium.

Results of experiments at different solid/liquid ratio are shown in Figures 6-8 and 6-9 and removal efficiencies are represented in Figure 6-10.
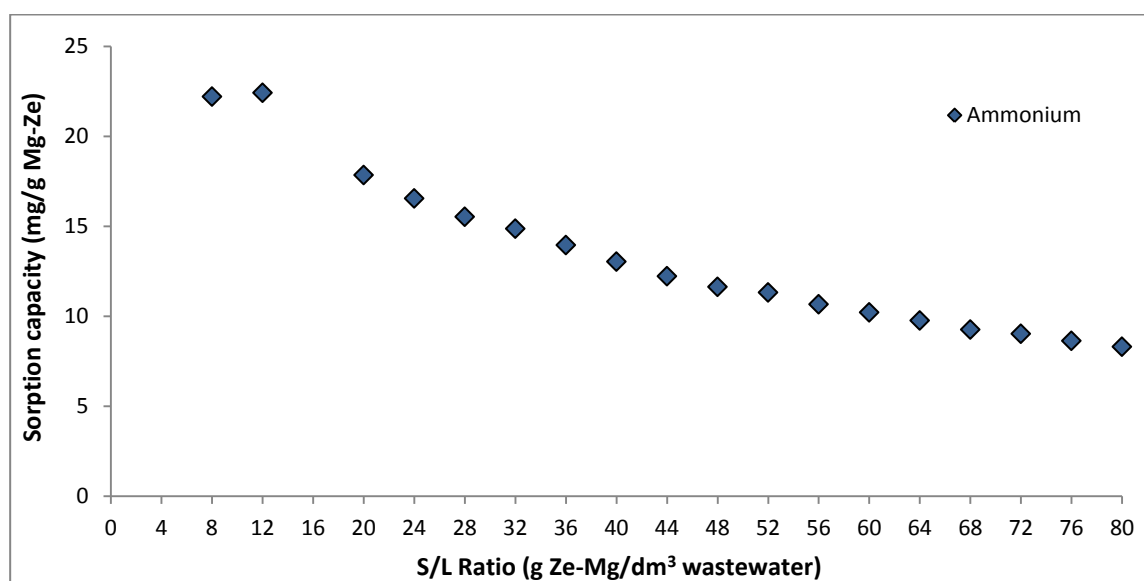

Figure 6-8. S/L ratio as a function of sorption capacity of Ze-Mg for ammonium
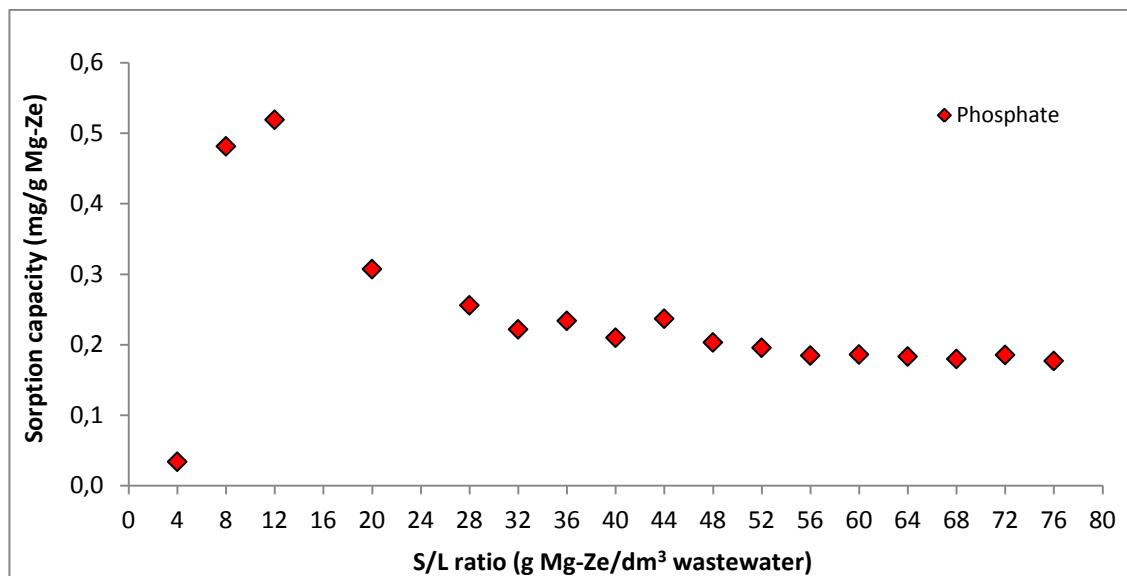
Figure 6-9. S/L ratio as a function of sorption capacity of Ze-Mg for phosphate
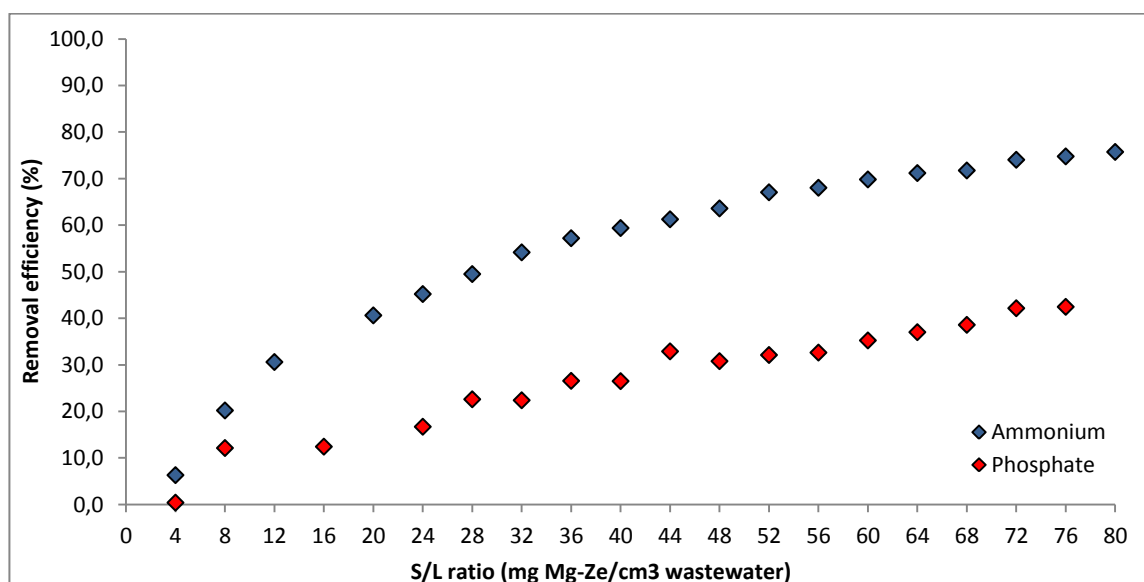
Figure 6-10. S/L ratio as a function of Mg-Ze removal efficiencies of ammonium and phosphate

Two main criteria were considered to select the optimum ratio solid/liquid: i) the sorption capacity of the zeolite (mg/g Mg-Ze) and ii) the removal efficiency of ammonium and phosphate (%).

Therefore, a relation of 32 g/L should be considered since contributes with the aimed minimum of 50% elimination of ammonium (Figure 6-10) as well as with a high sorption capacity (54 mg/g-Ze and 22 mg/g-Ze for ammonium and phosphate, respectively).

However, although it is desired to use the optimum solid/liquid ratio in further experiments at the pilot plant, it is actually not possible due to the work conditions of the plant. S/L ratio must be always between 1.0 and 2.5 g Ze/dm^3; that means a maximum of 100 g for each 40 liters of wastewater. The reason is indeed that the membrane may otherwise become saturated of zeolite and consequently damaged.

Thus, a new equilibrium study was carried out with lower S/L ratios, mixing the zeolite both with wastewater and synthetic water in different samples.
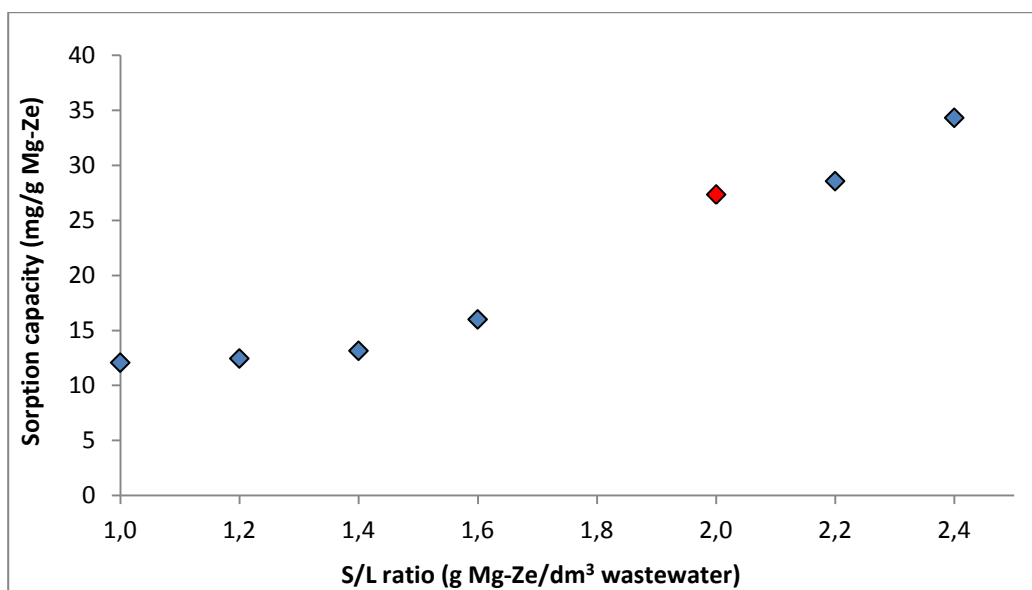
Figure 6-11. S/L ratio as a function of sorption capacity of Ze-Mg for ammonium
(S/L ratios between 1.0 and 2.5 g/dm^3)

It is noticeable the fact that increasing S/L ratio from 1.6 g/dm^3 to 2.0 g/dm^3 reported a significant increase of the sorption capacity (see Figure 6-10). Taking into account that with these lower S/L ratios is by far not possible achieving 50% of removal (see Figure 6-12). Thus, 2.0 g/dm^3 is considered a good enough S/L ratio in terms of sorption capacity; hence it has been selected as the optimum relation and has been decided to be used later on in the pilot plant experiments.
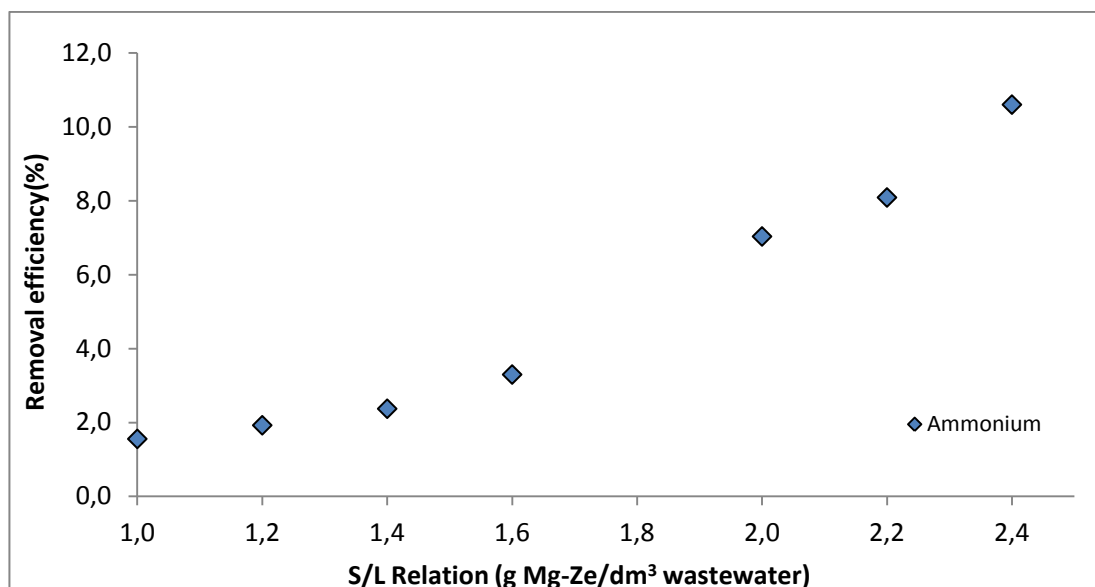
Figure 6-12. S/L ratio as a function removal efficiency of Ze-Mg for ammonium
(S/L ratios between 1.0 and 2.5 g/dm^3)

6.5. Hybrid UF-Sorption pilot plant performance

Tap water analysis reported in general low concentrations of all species, in comparison with the concentrations in the wastewater. The characterizations of tap water and wastewater are detailed in the Table 6-5.

Table 6-5. Characterization of tap water and desired concentrations (wastewater)

Species	Concentration in tap water (mg/dm^3)	Concentration in wastewater (mg/dm^3)
Na^+	21.1	~ 475
K^+	1.0	~ 60
Mg^{2+}	9.3	~ 90
Ca^{2+}	48.1	~ 400
NH_4^+	n.a.	~ 600
PO_4^{3-}	n.a.	~ 48
NO_3^-	2.4	~ 5
SO_4^{2-}	32.8	~ 5
Cl^-	21.7	~ 1200
HCO_3^-	158.6	~ 2000

After adding the corresponding salts to the tap water, the resulting solution was analyzed by chromatography, and it was shown that concentration values were very close to the

wastewater (Table 6-6), whereby it was considered to be successfully prepared and it proceeded to be used for the pilot plant application study.

Table 6-6. Characterization of the water solution prepared from tap water

Species	Concentration (mg/dm^3)
Na$^+$	478.9
K$^+$	57.2
Mg^{2+}	95.9
Ca^{2+}	430.7
NH$_4^+$	536.7
PO$_4^{3-}$	51.4
NO$_3^-$	2.8
SO$_4^{2-}$	31.3
Cl$^-$	2149.3
HCO$_3^-$	1659.6

Since the concentrate stream from UF unit was recirculated, ammonium and phosphate were accumulated in the system over time, so the concentration tended to increase. This fact involves an increase of the sorption capacity of the zeolite as well, as the sorption in the equilibrium is directly proportional to the concentration of the adsorbate.

Figures 6-13 and 6-14 support this argumentation as it can be observed that the zeolite sorption capacity tended to rise up over time.
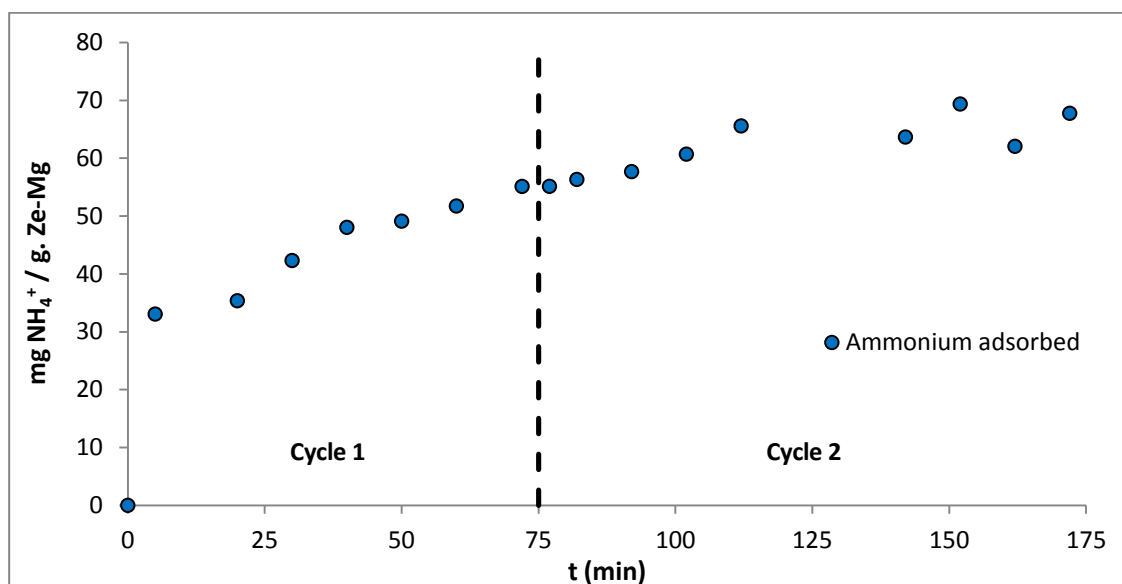
Figure 6-13. Ammonium adsorbed onto Ze-Mg over time in hybrid UF-sorption pilot plant
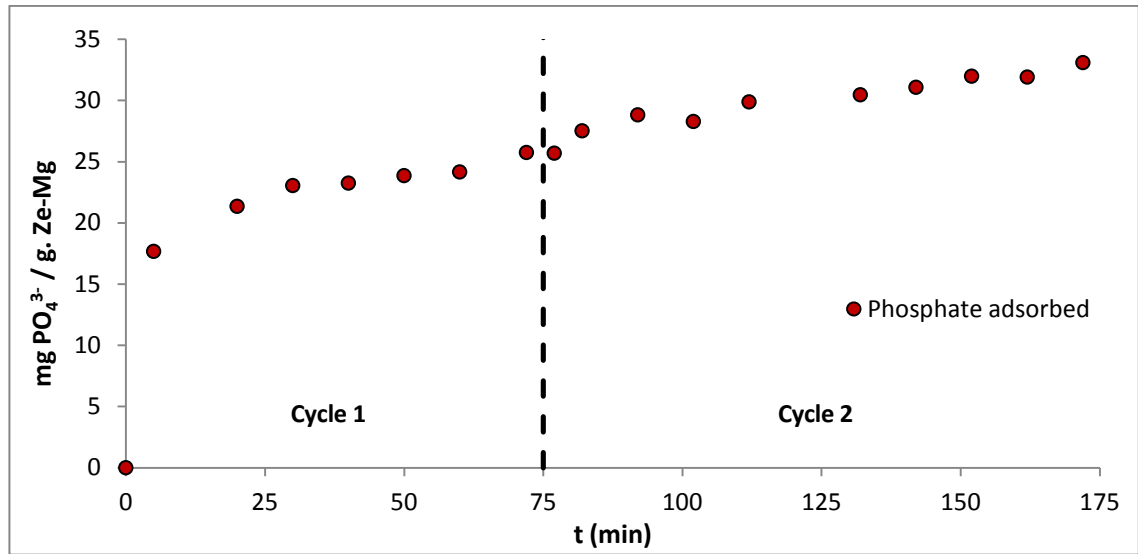
Figure 6-14. Phosphate adsorbed onto Ze-Mg over time in hybrid UF-sorption pilot plant

It is also important to highlight that, after two cycles, the zeolite did not reach its maximum sorption capacity yet, as it can be observed in Figures 6-12 and 6-13, so it is concluded that it would still able to sorb both ammonium and phosphate in further cycles.

Figures 6-15 and 6-16 show the removal efficiency of ammonium and phosphate from the STR respectively, in terms of mass and concentration.
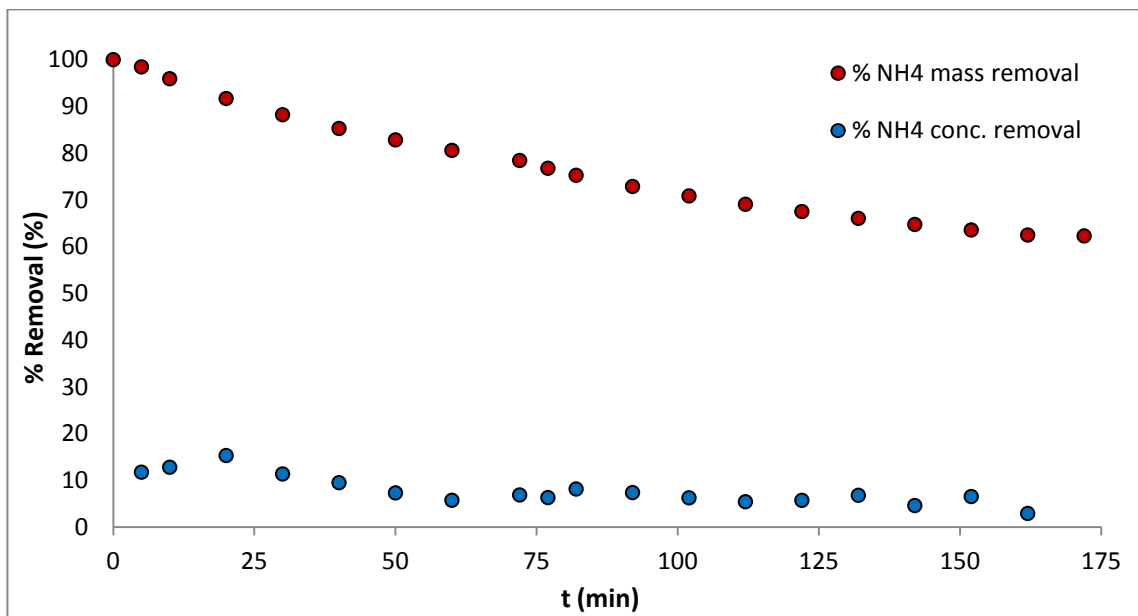
Figure 6-15. Removal efficiency of ammonium in terms of mass and concentration in hybrid UF-sorption pilot plant.
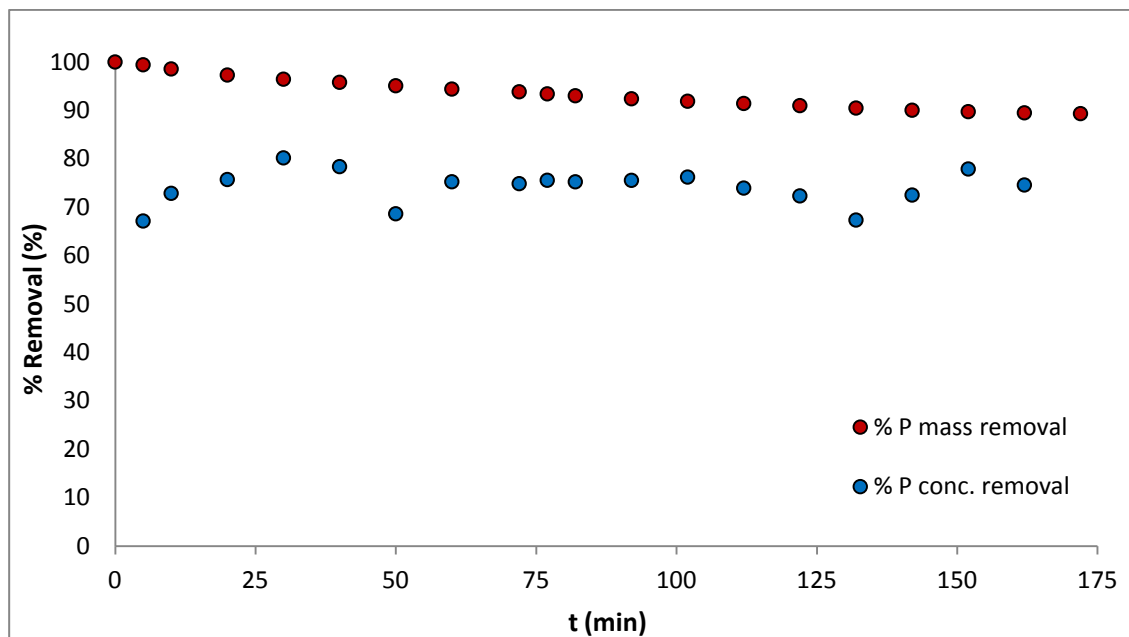
Figure 6-16. Removal efficiency of phosphate in terms of mass and concentration in hybrid UF-sorption pilot plant.

Ammonium removal is poor, up to 10-15% of concentration removal, but that was expected as the results fit well with the zeolite dose test reported in subsection 6.4. On the contrary, it is noteworthy the percentage of phosphate removed during the experiment, which ranges between 65-80 % of concentration. This is related to the high concentrations of Na^+ and Ca^{2+} in the solution, which trigger ionic exchange between this cations and the Mg^{2+} present on the zeolite surface, making struvite precipitation possible in a high quantity, and hence resulting in effective phosphate removal. Variations in the removal percentage are due to the fact that the STR level was difficult to maintain constant, and it permanently oscillated between 31.0 and 32.5 cm.

Finally, a comparison between the mass removal efficiency of ammonium and phosphate is shown in Figure 6-17.
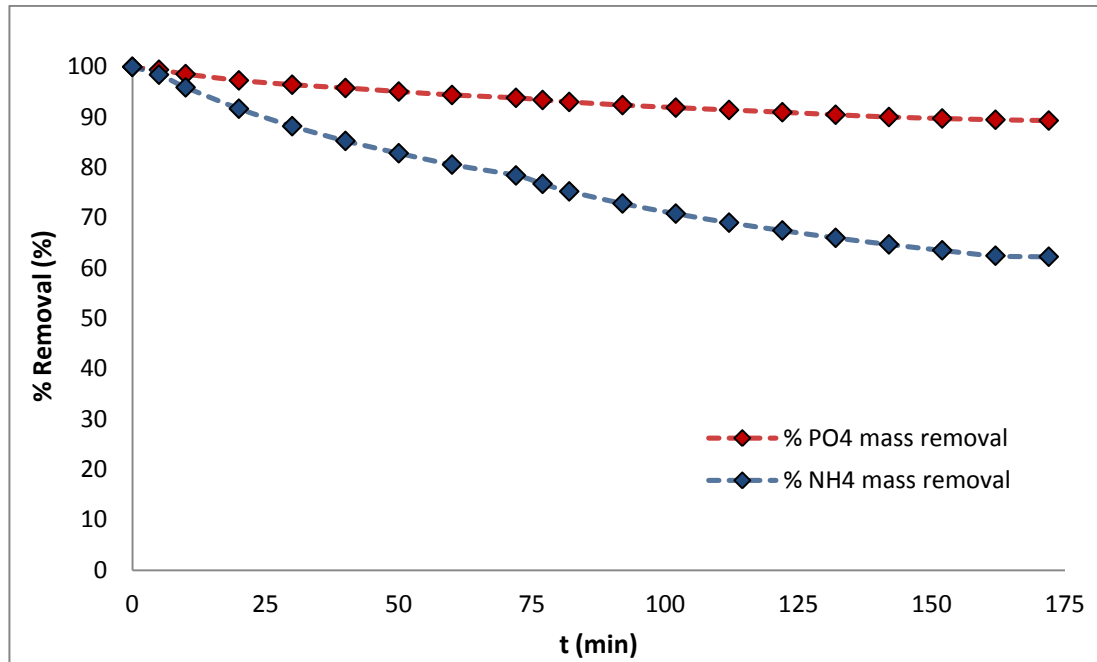
Figure 6-17. Comparison between NH_4^+ and PO_4^{3-} mass removal efficiency in hybrid UF-adsorption pilot plant

It is worth to point out that the system arrives to a stationary state after 3 hours of operation, when total mass removal efficiencies of NH_4^+ and PO_4^{3-} become constant at a specific value. It does not represent that zeolite is saturated, even though it means that, from then on, NH_4^+ and PO_4^{3-} of untreated input stream will be removed with the same efficiency (in terms of total mass) until the zeolite becomes actually saturated. At this point, mass removal efficiency will start falling down, and ammonium and phosphate will become indefinitely accumulated in the reactor tank over the time.

Results show that removal of phosphate stabilizes around 90% of mass removal, while ammonium does it around 60%. This means that permeate is coming out of the system with a 60% and 90% less of ammonium and phosphate respectively than its initial mass content.

ETSEIB

7. Environmental Impact Assessment

7.1. Impact at laboratory scale

During the performance of all the tests carried out as a part of this project, several wastes were generated. Table 7-1 collects information about these waste in every single experiment, as well as other pollutant factors.

Table 7-1. Pollutant sources generated during the present project

EXPERIMENT	ELEMENT
Zeolite modifications	Salt solutions and filter paper.
Equilibrium sorption studies	Loaded zeolites and salt solutions, and wasted syringe filters
Kinetic studies	Loaded zeolites and salt solutions, and wasted syringe filters
Zeolite dose studies	Loaded zeolites and salt solutions, and wasted syringe filters
Work at UF-adsorption pilot plant	High energy and water consumption, noise disturbance, loaded zeolites, salt solutions, and wasted syringe filters

Most relevant of these factors are liquid effluents and solid wastes.

Liquid effluents are all treated wastewater samples, which still contain high concentrations of organic compounds, ammonium and phosphate. In addition, they contain metal ions that were released by the zeolites during the adsorption process. This waste were separated into a specific deposit after every single experiment, in order to be treated afterwards by an external company according to the waste management rules of the department.

Solid wastes are basically loaded zeolites, which must be regenerated before being used again. To do so, it is necessary to bring them under a desorption process, which an external company is responsible of. Zeolite loaded samples were therefore separated into a container, after being dried in the oven at 50 ºC. As a solid waste there were also saturated syringe filters, which were kept and then brought under a backwash to recover the zeolite waste.

ETSEIB

7.2. Global scale impact assessment

7.2.1. Environment

Due to that the aim of this project is to recover nutrients that can be used as potential fertilizers, it can be considered that this study has a positive impact on the environment. Since no new pollutants are generated (wastewater comes from a wastewater treatment plant and zeolites are obtained from coal power plants), the environment is overall under improvements. In addition, the use of recovered nutrients as fertilizers reduces the dependence of exploiting our natural resources of phosphate rock, fact that helps to the preservation of the environment.

7.2.2. Society

The global society suffers the consequences of human activities. For that reason, all wastes generated at laboratory scale must be managed in an appropriate way so that the impact they can produce is perceived as less as possible. If this goal is successfully achieved, then the society will be exempt of those factors that may cause harmful consequences.

If use of zeolites is some day spread out to an industrial scale, fertilizers industry will be for sure a precursor of significant improvements in crop science and technology. This would also have a positive impact on the global society.

7.2.3. Economy

This project can be considered as low-cost since zeolites are collected from energy coal power plants. All the economical investment on this project is linked basically to labware and equipments. Comparing to other wastewater treatments, zeolites are much more economic.

Moreover, using zeolites as sorbent is a form of revaluating waste materials from other industrial processes and using them as a raw material, making this study potentially sustainable in terms of economical issues.

8. Economic study

This section presents the evaluation of the total expenses that were accounted to perform this project, by regarding at all the expenses are related to equipment, laboratory consumables, reagents, human resources and supply costs.

Equipment

The value of analysis and measurement equipment is calculated depending upon its amortization, according to Eq. 8-1.

$$Amortization\ [€] = \frac{Acquisition\ cost\ [€]}{Service\ life\ [years] \cdot \frac{12\ months}{1\ year}} \cdot period\ of\ use\ [months] \qquad \text{Eq. 8-1}$$

EQUIPMENT	Qty.	Cost/unit [€/u]	Total cost [€]	Service life [years]	Period used	Amortization [€]
Chromatograph Dionex ICS-1000	2	12,500	25,000	15	4 months	555.55
SEM/EDS system JEOL JSM-7001F	1	15,000	15,000	15	1 day	2.74
UF-adsorption pilot plant						
Masterflex® I/P Pump + accessories	1	3,000	3,000	15	1 week	4.17
Pentair® X-flow UF Membrane	1	subsidized	subsidized	5	1 week	-
Keller® Digital Manometer LEO3	2	640	1280	10	1 week	2.67
Legris® 100m polyurethane tubing	1	5	5	2	1 week	0.05
Legris® 3-way valves	6	25	150	5	1 week	0.62
Fittings and others	several	diverse	30	2	1 week	0.31
TOTAL						**566.11**

Some labware equipment like the magnetic multi-stirrer and the analytical balance are considered as already amortized.

Laboratory consumables

ITEM	Qty.	Cost/unit [€/u]	Total cost [€]
250 cm^3 beaker	10	2.19	21.90
600 cm^3 beaker	2	3.07	6.14
1000 cm^3 beaker	1	6.14	6.14
100 cm^3 volumetric flask	2	2.66	5.32
250 cm^3 volumetric flask	2	3.53	7.06
500 cm^3 volumetric flask	2	5.19	10.38
1000 cm^3 volumetric flask	1	7.67	7.67
5000 cm^3 volumetric flask	1	113.00	113.00
Filter paper (100 u/pack)	1	40.00	40.00
Parafilm roll 75 m	2	30.00	60.00
Micropipette 1-10 cm^3	1	280.00	280.00
Micropipette 0.5-5 cm^3	1	280.00	280.00
Tips for micropipette 1-10 cm^3	10	0.03	0.30
Tips for micropipette 0.5-5 cm^3	5	0.03	0.15
Syringes (100 u/box)	1	10.00	10.00
Syringe filters 0.2 µm (100 u/box)	1	79.00	79.00
Syringe filters 0.45 µm (100 u/box)	1	22.00	22.00
Stir bars	10	1.50	15.00
Spatula	1	5.00	5.00
Wash bottle 1 dm^3	1	3.00	3.00
Watch glass	2	5.00	10.00
TOTAL			**982.06**

Some of the used items as for example chromatography vials, 50cm^3 plastic bottles, 10 cm^3 polyethylene tubes and tube racks, are not counted within the total cost of the labware because they are plastic-made and are already amortized as they have been used for a long time in previous projects.

ETSEIB

Reagents

REAGENT	Qty.	Cost/unit [€/u]	Total cost [€]
NaCl (500 g)	2	22.00	44.00
$MgCl_2 \cdot 6H_2O$ (500 g)	2	43.30	86.60
$CaCl_2 \cdot 2H_2O$ (500 g)	1	26.00	26.00
KCl (500 g)	1	42.40	42.40
NH_4Cl (1 kg)	1	60.10	60.10
KNO_3 (500 g)	1	35.10	35.10
$NaHCO_3$ (500 g)	1	36.50	37.00
K_2HPO_4 (500 g)	1	39.70	39.70
$NaH_2PO_4 \cdot 2H_2O$ (500 g)	1	42.40	42.40
Milli-Q water (dm^3)	50	1.00	50.00
Zeolitic materials	**Mass [g]**	**Cost/gram [€/g]**	**Total cost [€]**
Zeolite NaP1	300	give-away	-
TOTAL			**463.30**

Human resources and supply costs

WORK	Time [h]	Salary [€/h]	Total cost [€]
Experimentation	450	10.00	4,500.00
Data analysis	300	8.00	2,400.00
SUPPLY	**Qty.**	**Unitary cost [€/m^3, €/kWh]**	**Total cost [€]**
Water	50 m^3	1.50	75.00
Energy	1000 kWh	0.15	150.00
TOTAL			**7,125.00**

Total cost of the project

CONCEPT	Cost [€]
Equipment	566.11
Laboratory consumables	982.06
Reagents	463.30
Human resources and supply costs	7,125.00
SUBTOTAL	**9136.47**
VAT (21 %)	**1918.66**
TOTAL NET COST	**11055**

ETSEIB

ETSEIB

9. Proposal for future work

As a continuation of this project, it would be interesting to keep on studying the performance of other zeolite forms. It would be important also to know in which stage of wastewater treatment at WWTP's would ammonium and phosphate removal be feasible, since further experiments at the UF-adsorption pilot plant are expected to be performed with real wastewater samples.

It would be also interesting to study how to carry out zeolite desorption in order to release adsorbed nutrients into the soil, and witness their effect on vegetation.

As suggestions for improvements, I would propose to attempt managing better the pilot plant experiments, by for example implementing a computerized system. Incorporating to the whole system an extern filter would help to enable real wastewater samples to be used with the UF membrane too.

ETSEIB

ETSEIB

Nutrient recovery from wastewater by adsorption on Magnesium/Potassium zeolites
in adsorption-ultrafiltration hybrid systems
Page 59

Conclusions

The conclusions that have been drawn from the results obtained in this study are presented below:

In the characterization of the zeolites carried out through SEM and EDS analysis, it is proven that the modifications of the initial zeolite (NaP1) to Mg-Ze and Mg/K-Ze forms were successful, although Mg^{2+} is not completely exchanged due to its low affinity with the zeolites surface. Thus, the Mg/K-Ze becomes basically a potassium modified form, while the Mg-Ze remains with still a high quantity of Na^+.

All equilibrium experimental data were well fitted by Langmuir isotherm model. Ammonium sorption capacity of both studied zeolites were similar (28 $mg \cdot g^{-1}$ on Mg/K-Ze and 31 $mg \cdot g^{-1}$ on Mg-Ze), while phosphate sorption capacity was higher on Mg/K-Ze than on Mg-Ze. (58 $mg \cdot g^{-1}$ and 12 $mg \cdot g^{-1}$, respectively). However, Mg-Ze reported to have a higher magnesium composition (%) than Mg/K-Ze and it might trigger struvite (MAP) crystallization, which is an element of interest. For that reason, zeolite dose studies and pilot plant works were performed using the Mg-Ze.

Kinetics experimental data of the Mg/K-Ze sorption mechanism were fitted well with the pseudo-second order model. The solid/liquid ratio studies carried out showed that the optimum S/L ratio depended on the volume of the samples and the concentration of NH_4^+ and PO_4^{3-} on water. However, only doses within the range between 1.0 and 2.5 g/dm^3 were considered due to the UF pilot plant restrictions concluding that the optimum S/L ratio to be used at the UF-adsorption pilot plant was 2.0 g/dm^3.

Finally, during the experiment carried out Mg-Ze demonstrated to have its maximum sorption capacity beyond 70 $mg \cdot g^{-1}$ and 30 $mg \cdot g^{-1}$ for ammonium and phosphate, respectively. The zeolites did not reach saturation at any moment of the experiment, so their sorption capacities are even higher than last sorption values reported. Moreover, when working in continuous reactor, ammonium mass removal efficiency stabilized at 60% and phosphate mass removal did so at 90%. These values were reached after 3 hours of continuous reaction in the STR.

ETSEIB

ETSEIB

Acknowledgements

First of all, I would like to give my gratitude to César A. Valderrama and José L. Cortina for showing their confidence in me and giving me the opportunity and the means to realize my bachelor degree project.

In second place, I feel the need to give special thanks to Xialei You for giving me her full support and help during these 5 months. I will be eternally indebted to her for her patience and dedication, and also for being so friendly and having such a close deal with me.

Also thanks to the rest of PhD students: Marc, Mónica, Neus, Sandra, and especially Mehrez. They have given me lots of good advices and they encouraged me to work hard on this. I wish them all the best.

Finally, I want to thank my family and my friends for supporting me at this stage of my career.

ETSEIB

Nutrient recovery from wastewater by adsorption on Magnesium/Potassium zeolites
in adsorption-ultrafiltration hybrid systems

Page 63

References

Ashrafizadeh, S.N., Khorasani, Z., Gorjiara, M. (2008). Ammonia removal from aqueous solutions by Iranian natural zeolite. *Separation Science and Technology, 43,* 960-978.

Aoudj, S., Khelifa, A., Drouiche, N., Belkada, R., Miroud, D. (2015). Simultaneous removal of chromium(VI) and fluoride by electrocoagulation–electroflotation: Application of a hybrid Fe-Al anode. *Chemical Engineering Journal, 267,* 153-162.

Azmi, N.S., Yunos, K.F. (2014). Wastewater Treatment of Palm Oil Mill Effluent (POME) by Ultrafiltration Membrane Separation Technique Coupled with Adsorption Treatment as Pre-treatment. *Agriculture and Agricultural Science Procedia, 2,* 257-264.

Bi, W., Li, Y., Hu, Y. (2014). Recovery of phosphorus and nitrogen from alkaline hydrolysis supernatant of excess sludge by magnesium ammonium phosphate. *Biosource Technology, 166,* 1-8.

Cagdas Ozturk, M., Martin Serrat, F., Teymour, F. (2015). Optimization of aeration profiles in the activated sludge process. *Chemical Engineering Science, 139,* 1-14.

Crini, G. (2005). Recent developments in polysaccharide-based materials used as adsorbents in wastewater treatment. *Progress in Polymer Science, 30*, 38-70.

Feng-Chin Wu, Ru-Ling Tseng, Ruey-Shin Juang (2009). Characteristics of Elovich equation used for the analysis of adsorption kinetics in dye-chitosan systems. *Chemical Engineering Journal, 150,* 366-373.

Galera, M. (2015). Phosphate recovery by synthetic zeolite and fly-ash: sorption characterization and performance assessment in hybrid sorption-ultrafiltration pilot plant. *Universitat Politècnica de Catalunya*.

Guo, X.J., Zeng, L., Li, X.M., Park, H.S. (2007). Removal of ammonium from RO permeate of anaerobically digested wastewater by natural zeolite. *Separation Science and Technology, 42,* 3169-3185.

ETSEIB

Guzmán, A., Nava, J.L., Coreño, O., Rodríguez, I., Gutiérrez, S. (2016). Arsenic and fluoride removal from groundwater by electrocoagulation using a continuous filter-press reactor. *Chemosphere, 144,* 2113-2120.

Ho, Y.S., McKay, G. (1999). Pseudo-second order model for sorption processes. *Process Biochemistry, 34,* 451-465.

Huang, H., Jiang, Y., Ding, L. (2014). Recovery and removal of ammonia-nitrogen and phosphate from swine wastewater by internal recycling of struvite chlorination product. *Biosource Technology, 172,* 253-259.

Huang, H., Xiao, D., Pang, R., Han, C., Ding, L. (2014). Simultaneous removal of nutrients from simulated swine wastewater by adsorption of modified zeolite combined with struvite crystallization. *Chemical Engineering Journal, 256,* 431-438.

Idris, S., Iyaka, Y.A., Ndamitso, M.M., Mohammed, E.B., Umar, M.T. (2011). Evaluation of Kinetic Models of Copper and Lead Uptake from Dye Wastewater by Activated Pride of Barbados Shell. *American Journal of Chemistry, 1(2),* 47-51.

Inyang, H., Onwawoma, A., Bae, S. (2015). The Elovich equation as a predictor of lead and cadmium sorption rates on contaminant barrier minerals. *Soil & Tillage Research, 155,* 124-132.

Ji, X., Zhang, M., Wang, Y., Song, Y., Ke, Y., Wang, Y. (2015). Immobilization of ammonium and phosphate in aqueous solution by zeolites synthesized from fly ashes with different compositions. *Journal of Industrial and Engineering Chemistry, 22,* 1-7.

Karadag, D., Koc, Y., Turan, M., Ozturk, M. (2007). A comparative study of linear and nonlinear regression analysis for ammonium exchange by clinoptilolite zeolite. *Journal of Hazardous Materials, 144,* 432-437.

Kim, J., Park, M., Shon, H.K., Kim, J.H. (2016). Performance analysis of reverse osmosis, membrane distillation, and pressure-retarded osmosis hybrid processes. *Desalination, 380,* 85-92.

Nutrient recovery from wastewater by adsorption on Magnesium/Potassium zeolites
in adsorption-ultrafiltration hybrid systems

Page 65

Kochany, J., Lipczynska-Kochany, E. (2009). Utilization of landfill leachate parameters for pretreatment by Fenton reaction and struvite precipitation—A comparative study. *Journal of Hazardous Materials, 166,* 248-254.

Koppelaar, R.H.E.M., Weikard, H.P. (2013). Assessing phosphate rock depletion and phosphorus recycling options. *Global Environmental Change, 23,* 1454-1466.

Li, X.Z., Zhao, Q.L. (2003). Recovery of ammonium-nitrogen from landfill leachate as a multi-nutrient fertilizer. *Ecological Engineering, 20,* 171-181.

Li, X., Lu, Y., He, Z. (2015). Removal of reverse-fluxed ammonium by anammox in a forward osmosis system using ammonium bicarbonate as a draw solute. *Journal of Membrane Science, 495,* 424-430.

Liu, C.H., Lo, K.V. (2001). Ammonia removal from composting leachate using zeolite. I. Characterization of the zeolite. J*ournal of Environmental Science and Health Part A: Toxic/Hazardous Substances & Environmental Engineering, 36,* 1671-1688.

López-Roldán, R., Rubalcaba, A., Martin-Alonso, J., González, S., Martí, V., Cortina, J.L. (2016). Assessment of the water chemical quality improvement based on human health risk indexes: Application to a drinking water treatment plant incorporating membrane technologies. *Science of the Total Environment, 540,* 334-343.

Luo, W., Hai, F.I., Price, W.E., Guo, W., Ngo, H.H., Yamamoto, K., Nghiem, L.D. (2016). Phosphorus and water recovery by a novel osmotic membrane bioreactor–reverse osmosis system. *Biosource Technology, 200,* 297-304.

Ma, B., Wang, S., Cao, S., Miao, Y., Jia, F., Du, R., Yongzhen, P. (2016). Biological nitrogen removal from sewage via anammox: Recent advances. *Biosource Technology, 200,* 981-990.

Mailler, R., Gasperi, J.,Coquet, Y., Buleté, A., Vulliet, E., Deshayes, S., Zedek, S., Mirande-Bret, C., Eudes, V., Bressy, A., Caupos, E., Moilleron, R., Chebbo, G., Rocher, V. (2016). Removal of a wide range of emerging pollutants from wastewater treatment plant discharges by micro-grain activated carbon in fluidized bed as tertiary treatment at large pilot scale. *Science of the Total Environment, 542, 983-996.*

ETSEIB

Mukherjee, R., De, S. (2016). Novel carbon-nanoparticle polysulfone hollow fiber mixed matrix ultrafiltration membrane: Adsorptive removal of benzene, phenol and toluene from aqueous solution. *Separation and Purification Technology, 157,* 229-240.

Osman, A., Gringer, N., Svendsen, T., Yuan, LF., Hosseini, S.V., Baron, C.P., Undeland, I. (2015). Quantification of biomolecules in herring (Clupea harengus) industry processing waters and their recovery using electroflocculation and ultrafiltration. *Food and Bioproducts Processing, 96,* 198-210.

Qiu, D. (2015). Characterization of ammonium and phosphate adsorption by synthetic zeolite. *Universitat Politècnica de Catalunya*.

Querol, X., Moreno, N., Umaña, J.C., Alastuey, A., Hernández, H., López-Soler, A., Plana, F. (2002). Synthesis of zeolites from coal fly ash: an overview. *International Journal of Coal Geology, 50,* 413-423.

Querol, X., Moreno, N., Alastuey, A., Juan, R., Andrés, J.M., López-Soler, A., Ayora, C., Medinacelli, A., Valero, A. (2007). Synthesis of high ion exchange zeolites from coal fly ash. *Geologica Acta, 5(1),* 49-57.

Robati, D. (2013). Pseudo-second-order kinetic equations for modeling adsorption systems for removal of lead ions using multi-walled carbon nanotube. *Journal of Nanostructure in Chemistry,* 3:55.

Rozic, M., Cerjan-Stefanovic, S., Kurajica, S., Vancina, V., Hodzic, E. (2000). Ammoniacal nitrogen removal from water by treatment with clays and zeolites. *Water Research, 34,* 3675-3681.

Shu, L., Schneider, P., Jegatheesan, V., Johnson, J. (2006). An economic evaluation of phosphorus recovery as struvite from digester supernatant. *Biosource Technology, 97,* 2211-2216.

Song, Y., Yuan, P., Zheng, B., Peng, J., Yuan, F., Gao, Y. (2007). Nutrients removal and recovery by crystallization of magnesium ammonium phosphate from synthetic swine wastewater. *Chemosphere, 69,* 319-324.

Nutrient recovery from wastewater by adsorption on Magnesium/Potassium zeolites
in adsorption-ultrafiltration hybrid systems

Page 67

Tilman, D., Fargione, J., Wolff, B., D'Antonio, C., Dobson, A., Howarth, R., Schindler, D., Schlesinger, W.H., Simberloff, D., Swackhamer, D. (2001). Forecasting Agriculturally Driven Global Environmental Change. *Science, 292,* 281-284.

Tseng, R.L., Wu, F.C., Juang, R.S. (2010). Characteristics and applications of the Lagergren's first-order equation for adsorption kinetics. *Journal of the Taiwan Institute of Chemical Engineers, 41,* 661-669.

US Geological Survey, 2015. Phosphate rock. Available from:
http://minerals.er.usgs.gov/minerals/pubs/commodity/phosphate_rock/mcs-2015-phosp.pdf

Vadivelu, Vel M., Keller, J., Yuan, Z. (2007). Effect of free ammonia on the respiration and growth processes of an enriched Nitrobacter culture. *Water research, 41,* 826-834.

Van Vuuren, D.P., Bouwman, A.F., Beusen, A.H.W. (2010). Phosphorus demand for the 1970–2100 period: A scenario analysis of resource depletion. *Global Environmental Change, 20,* 428-439.

Wang, S., Wu, H. (2006). Environmental-benign utilisation of fly ash as low-cost adsorbents. *Journal of Hazardous Materials, 136,* 482-501.

Wang, Y.F., Lin, F., Pang, W.Q. (2007). Ammonium exchange in aqueous solution using Chinese natural clinoptilolite and modified zeolite. *Journal of Hazardous Materials, 142,* 160-164.

Wang C., Li, J., Sun, X., Wang, L., Sun, X. (2009). Evaluation of zeolites synthesized from fly ash as potential adsorbents for wastewater containing heavy metals. *Journal of Environmental Sciences, 21,* 127-136.

Wang, H., Qu, F., Ding, A., Liang, H., Jia, R., Li, K., Bai, L., Chang, H., Li, G. (2016). Combined effects of PAC adsorption and in situ chlorination on membrane fouling in a pilot-scale coagulation and ultrafiltration process. *Chemical Engineering Journal, 283,* 1374-1383.

Wang, S., Peng, Y. (2010). Natural zeolites as effective adsorbents in water and wastewater treatment. *Chemical Engineering Journal, 156,* 11-24.

Warmadewanthi, Liu, J.C. (2009). Recovery of phosphate and ammonium as struvite from semiconductor wastewater. *Separation and Purification Technology, 64,* 368-373.

Weatherley, L.R., Miladinovic, N.D. (2004). Comparison of the ion exchange uptake of ammonium ion onto New Zealand clinoptilolite and mordenite. *Water Research, 38,* 4305-4312.

Widiastuti, N., Wu, H., Ming Hang, H., Zhang, D. (2011). Removal of ammonium from greywater using natural zeolite. *Desalination, 277,* 15-23.

Wu, D., Zhang, B., Li, C., Zhang, Z., Kong, H. (2006). Simultaneous removal of ammonium and phosphate by zeolite synthesized from fly ash as influenced by salt treatment. *Journal of Colloid and Interface Science, 304,* 300-306.

Wu, D., Hu, Z., Wang, X., He, S., Kong, H. (2007). Use of zeolitized coal fly ash in the simultaneous removal of ammonium and phosphate from aqueous solution. *Frontiers of Environmental Science & Engineering in China, 1(2),* 123-220.

Xie, Y., Li, S., Wu, K., Wang, J., Liu, G. (2011). A hybrid adsorption/ultrafiltration process for perchlorate removal. *Journal of Membrane Science, 366,* 237-244.

Yang, M., Lin, J., Zhan, Y., Zhang, H. (2014). Adsorption of phosphate from water on lake sediments amended with zirconium-modified zeolites in batch mode. *Ecological Engineering, 71,* 223-233.

Zhang, F., Li, J., He, Z. (2014). A new method for nutrients removal and recovery from wastewater using a bioelectrochemical system. *Biosource Technology, 166,* 630-634

Zhang, M., Zhang, H., Xu, D., Han, L., Niu, D., Zhang, L., Wu, W., Tian, B. (2011). Ammonium removal from aqueous solution by zeolites synthesized from low-calcium and high-calcium fly ashes. *Desalination, 277,* 46-53.

Zhang, T., Ding, L., Ren, H., Guo, Z., Tan, J. (2010). Thermodynamic modeling of ferric phosphate precipitation for phosphorus removal and recovery from wastewater. *Journal of Hazardous Materials*, *176*, 444-450.